

Vector boson production in hadronic collisions

R.K. Ellis

Theory Group, Fermi National Accelerator Laboratory, P.O. Box 500, Batavia, IL 60510

D.A. Ross

Physics Department, University of Southampton, UK

Siniša Veseli

Theory Group, Fermi National Accelerator Laboratory, P.O. Box 500, Batavia, IL 60510

May 13, 2019

Abstract

We consider the production of γ^* , W and Z vector bosons in hadron-hadron collisions in perturbative QCD. We present results from a new numerical program which gives a full description of the production of the vector bosons and of their decay products. At small q_T the calculation includes resummation of large logarithms and non-perturbative effects. The resummation is matched with the full $O(\alpha_S)$ calculation. In addition, the program correctly reproduces the known $O(\alpha_S)$ cross section when integrated over q_T . Besides presenting results for W and Z production at the Tevatron, we also review constraints on the non-perturbative functions using fixed target data on lepton pair production, and make several observations on this topic.

1 Introduction

The aim of this paper is to give a complete description of the leptons coming from the decay of a vector boson produced in hadron-hadron collisions. In addition to the intrinsic interest of obtaining a complete description of vector boson production, a precise measurement of the W mass at a hadronic collider will depend on accurate theoretical information about its production properties. Since it is the leptonic decay products of the vector bosons which are actually observed, it is important to include the decay so that experimental cuts can be implemented. Leptons produced at large transverse momenta can come from vector bosons having either large or small q_T , where q_T is the transverse momentum of the vector boson. It is therefore essential to use a formalism which is valid for both large and small transverse momentum of the vector bosons.

The production of vector bosons at large and small q_T has been extensively considered before. Vector bosons at large q_T attracted early interest because they provided discrimination between the naive parton model (which predicts a limitation on q_T) and an underlying field theory (which predicts events at large q_T). The transverse momentum of a vector boson recoiling against one parton was calculated in Ref. [1]. The $O(\alpha_S^2)$ calculation of vector boson production at large q_T was initiated in Ref. [2] and completed in Refs. [3] and [4]. These papers on the q_T distribution give no information on the distribution of the leptons into which the vector bosons decayed. This deficiency was remedied in Ref. [5] for the $O(\alpha_S)$ case and in Refs. [6, 7] for the $O(\alpha_S^2)$ case.

However the bulk of the data is not at large q_T . At small q_T order by order in perturbation theory we encounter large logarithms of Q^2/q_T^2 , where Q is the vector boson mass. For example, at small q_T the leading term in the cross section is of the form

$$\frac{d\sigma}{dq_T^2} \sim \frac{\alpha_S}{q_T^2} \ln \frac{Q^2}{q_T^2} . \quad (1)$$

The logarithms can be resummed to give a Sudakov form factor [8, 9]. The resummation has a simple exponential form after transformation to the impact parameter, b , which is the Fourier conjugate of q_T [9]. The necessary coefficients for the inclusion of higher order

terms in the resummation were calculated in Ref. [10] using the results of Ref. [2]. The formalism which we shall use was written down in Ref. [11] using techniques developed earlier for back-to-back jets [12]. Numerical results of resummed calculations have been reported in Refs. [13, 14].

In order to have a complete description of the transverse momentum one must match the theoretical results at large and small q_T . The matching of the vector boson cross section including $O(\alpha_S)$ has been considered in Ref. [13]. The matching including the full $O(\alpha_S^2)$ calculation appropriate at large q_T is given in Ref. [15]. The papers in Ref. [16] have combined fixed order calculations with a parton shower approach.

One of the most interesting results of the resummation procedure is that for large enough vector boson mass perturbation theory is valid even at $q_T = 0$. In fact, using the saddle point method it is found [9, 11] that the Fourier transform integral to recover the transverse momentum distribution is determined (at $q_T = 0$) by an impact parameter of order

$$b_{\text{SP}} = \frac{1}{\Lambda} \left(\frac{\Lambda}{Q} \right)^\kappa, \quad (2)$$

where $\kappa = 16/(49 - 2n_f)$. Choosing $Q = M_W = 80.33$ GeV, $\Lambda = 250$ MeV and the number of active flavours $n_f = 5$ we find that the saddle point is at the position

$$b_{\text{SP}}^{-1} \approx 10\Lambda. \quad (3)$$

Thus for W and Z production the integral is dominated by values of b which are at the borderline between the perturbative and non-perturbative region. Detailed predictions therefore depend both on the perturbative Sudakov form factor and on a parametrization of the non-perturbative part of the form factor, to be extracted from data. The effect of non-perturbative terms on the vector boson q_T distribution has been considered in Refs. [14, 17, 18].

A treatment of the production of vector bosons including both the resummation at small transverse momentum and the decay kinematics has been given in [19]. In this paper we carry the analysis further and correct minor mistakes in Ref. [19]. A more

complete theoretical description could be obtained if the order α_S^2 were included at large q_T , (*i.e.* by extending the results of Arnold and Kauffman [15] to include the decay of the vector boson).

In Section 2 we give a brief summary of the formalism which we use for the theoretical description of vector boson cross production. Section 3 presents results for the $O(\alpha_S)$ q_T -integrated cross-section. Section 4 contains our numerical results. Besides discussing W and Z production, we also review the available information on the non-perturbative parameters which are important at low q_T , and point out several issues which have not been addressed previously in the literature. Our q_T -dependent predictions are obtained and verified using two independent programs based on the formalism of Section 2. For the q_T -integrated distributions we have implemented a separate program based on the results of Section 3. Our conclusions are presented in Section 5, while details of the formulae used in our numerical programs are given in two appendices.

2 Resummed cross section at hadron level

In the Collins-Soper frame¹ [20] the general expression for the resummed differential cross section at hadron level may be written in the form

$$\frac{d\sigma(AB \rightarrow V(\rightarrow l\bar{l}')X)}{dq_T^2 dQ^2 dy d\cos\theta d\phi} = \frac{1}{2^8 N\pi S} \frac{Q^2}{(Q^2 - M_V^2)^2 + M_V^2 \Gamma_V^2} \times \left[Y_r(q_T^2, Q^2, y, \theta) + Y_f(q_T^2, Q^2, y, \theta, \phi) \right]. \quad (4)$$

In the above, $N = 3$ is the number of colors, \sqrt{S} is the total hadron-hadron center-of-mass energy, while θ and ϕ refer to the lepton polar and azimuthal angles. The functions Y_r and Y_f stand for the resummed and finite² parts of the cross section, respectively. They are defined in the following subsections.

¹The Collins-Soper frame (defined in the Appendix A) is the rest frame of the vector boson with a specific choice for orientation.

²The “finite” part is integrable as $q_T^2 \rightarrow 0$ and contains no distributions.

2.1 Resummed part

The resummed part of the cross section is given as the Fourier integral over the impact parameter b ,

$$Y_r(q_T^2, Q^2, y, \theta) = \frac{1}{2\pi} \int b db J_0(q_T b) \sum'_{a,b} F_{ab}^{NP}(Q, b, x_A, x_B) \times W_{ab}(Q, b_*, \theta) f'_{a/A}(x_A, \mu(b_*)) f'_{b/B}(x_B, \mu(b_*)) . \quad (5)$$

In this expression the function F^{NP} represents the non-perturbative part of the form factor. Its specific form, as well as the definition of the variable b_* will be described below. The variables x_A and x_B are given in terms of the vector boson mass Q and rapidity y as

$$x_A = \frac{Q}{\sqrt{S}} \exp(y) , \quad x_B = \frac{Q}{\sqrt{S}} \exp(-y) . \quad (6)$$

Note that

$$\tau = x_A x_B = Q^2/S . \quad (7)$$

The modified parton structure functions f' are related to the \overline{MS} structure functions f by a convolution,

$$f'_{a/A}(x_A, \mu) = \sum_c \int_{x_A}^1 \frac{dz}{z} C_{ac}\left(\frac{x_A}{z}, \mu\right) f_{c/A}(z, \mu) , \quad (8)$$

where $(a, b \neq g)$ [10]

$$C_{ab}(z, \mu) = \delta_{ab} \left\{ \delta(1-z) + \frac{\alpha_S(\mu)}{2\pi} C_F \left[1-z + \left(\frac{\pi^2}{2} - 4\right) \delta(1-z) \right] \right\} , \quad (9)$$

$$C_{ag}(z, \mu) = \frac{\alpha_S(\mu)}{2\pi} T_R [2z(1-z)] . \quad (10)$$

In the above the colour factors are $C_F = 4/3$ and $T_R = 1/2$, while the prime on the sum in Eq. (5) indicates that gluons are excluded from the summation.

The function W from Eq. (5) can be written in terms of the the Sudakov form factor \mathcal{S} as

$$W_{ab}(Q, b, \theta) = \exp[\mathcal{S}(b, Q)] H_{ab}^{(0)}(\theta) . \quad (11)$$

The exact definition of the Sudakov form factor will be discussed below. The function $H^{(0)}$, which includes the angular dependence of the lowest order cross section and coupling factors, is defined in Appendix A.

2.1.1 Sudakov form factor, large and small b

In the formalism of Ref. [11] the Sudakov form factor $\mathcal{S}(b, Q)$ is given by

$$\mathcal{S}(b, Q) = - \int_{b_0^2/b^2}^{Q^2} \frac{d\bar{\mu}^2}{\bar{\mu}^2} \left[\ln \left(\frac{Q^2}{\bar{\mu}^2} \right) A(\alpha_s(\bar{\mu})) + B(\alpha_s(\bar{\mu})) \right] , \quad (12)$$

with $b_0 = 2 \exp(-\gamma_E) \approx 1.1229$. The coefficients A and B are perturbation series in α_S ,

$$A(\alpha_S) = \sum_{j=1}^{\infty} \left(\frac{\alpha_S}{2\pi} \right)^j A^{(j)} , \quad B(\alpha_S) = \sum_{j=1}^{\infty} \left(\frac{\alpha_S}{2\pi} \right)^j B^{(j)} , \quad (13)$$

where the first two coefficients in the expansion are known [10]:

$$\begin{aligned} A^{(1)} &= 2C_F , \\ A^{(2)} &= 2C_F \left(N \left(\frac{67}{18} - \frac{\pi^2}{6} \right) - \frac{10}{9} T_R n_f \right) , \\ B^{(1)} &= -3C_F , \\ B^{(2)} &= C_F^2 \left(\pi^2 - \frac{3}{4} - 12\zeta(3) \right) + C_F N \left(\frac{11}{9} \pi^2 - \frac{193}{12} + 6\zeta(3) \right) \\ &\quad + C_F T_R n_f \left(\frac{17}{3} - \frac{4}{9} \pi^2 \right) . \end{aligned} \quad (14)$$

In the above we take n_f to be the number of quark flavors active at the the scale at which α_S is evaluated. In addition, the formalism of Ref. [11] requires that the scale at which the parton distributions are evaluated in Eq. (5) is

$$\mu(b) = b_0/b . \quad (15)$$

Equations (12) through (15) should be compared with the exact first order results [13] for the Sudakov form factor,

$$\mathcal{S}(b, Q) = \frac{\alpha_S}{2\pi} C_F \int_0^{Q^2} \frac{d\bar{\mu}^2}{\bar{\mu}^2} \left[2 \ln \left(\frac{Q^2}{\bar{\mu}^2} \right) - 3 \right] [J_0(b\bar{\mu}) - 1] , \quad (16)$$

and for the scale $\mu(b)$,

$$\mu(b) = Q \exp \left\{ - \int_0^Q \frac{dx}{x} [1 - J_0(bx)] \right\}. \quad (17)$$

Formally, the integration over b in Eq. (5) is from 0 to ∞ . However, as b approaches $1/\Lambda$, the coupling α_S becomes large and the perturbative calculation of the form factor \mathcal{S} is no longer reliable. This region is effectively removed from the integral by evaluating W and the parton structure functions at

$$b_* = \frac{b}{\sqrt{1 + (b/b_{\text{lim}})^2}}, \quad (18)$$

which never exceeds the cut-off value b_{lim} . The large b part of the Sudakov form factor is provided by the function F^{NP} which parametrizes the non-perturbative effects [10, 11, 14]. The specific form of F^{NP} , as well as our results with particular choices for non-perturbative parameters, will be discussed in Section 4.

The formalism of Ref. [11] leaves open the question of small b . The small b -region does not contribute large logarithms, but a correct treatment is important to recover the total cross section after integration over q_T . The lowest order expression of Eq. (16) had the property that $\mathcal{S} \rightarrow 0$ as $b \rightarrow 0$, which is lost in Eq. (12). In Ref. [21] it has been suggested that one make the replacement in Eq. (12)

$$\left(\frac{b_0}{b}\right)^2 \rightarrow \left(\frac{b_0}{b}\right)^2 \frac{1}{[1 + b_0^2/(b^2 Q^2)]}, \quad (19)$$

This ensures that the scale never exceeds Q by adding power suppressed terms of order $(q_T/Q)^2$.

However, we shall use a slightly more sophisticated treatment which ensures that the first-order fixed-coupling result is correctly reproduced. We define scales λ and μ by

$$\int_\lambda^Q \frac{dx}{x} \ln\left(\frac{Q}{x}\right) = \int_0^Q \frac{dx}{x} \ln\left(\frac{Q}{x}\right) [1 - J_0(bx)], \quad (20)$$

$$\int_\mu^Q \frac{dx}{x} = \int_0^Q \frac{dx}{x} [1 - J_0(bx)], \quad (21)$$

which results in

$$\mu(b) = Q \exp \left\{ - \int_0^Q \frac{dx}{x} [1 - J_0(bx)] \right\}, \quad (22)$$

$$\lambda(b) = Q \exp \left\{ - \left[2 \int_0^Q \frac{dx}{x} \ln \left(\frac{Q}{x} \right) [1 - J_0(bx)] \right]^{\frac{1}{2}} \right\}. \quad (23)$$

Figure 1 shows λ and μ plotted for $Q = 5$ and 100 GeV. At large $b \gg 1/Q$ where the resummation is mandatory, we have that

$$\lambda, \mu \sim \frac{b_0}{b}, \quad (24)$$

in accordance with Eq. (12) and the procedure of Ref. [11]. In addition we have that $\mu(b), \lambda(b) \leq Q$, where the equality is true for $b = 0$.

Therefore, instead of Eq. (12) for the resummed form factor we shall use

$$\mathcal{S}(b, Q) = - \left[\int_{\lambda^2(b)}^{Q^2} \frac{d\bar{\mu}^2}{\bar{\mu}^2} \ln \left(\frac{Q^2}{\bar{\mu}^2} \right) A(\alpha_s(\bar{\mu})) + \int_{\mu^2(b)}^{Q^2} \frac{d\bar{\mu}^2}{\bar{\mu}^2} B(\alpha_s(\bar{\mu})) \right]. \quad (25)$$

For fixed coupling constant this expression is exactly in agreement with the lowest order result of Eq. (16), but also preserves the good features of Eq. (12). The exponential of the Sudakov form factor with this prescription is shown in Figure 2 for $Q = 5, 10$ and 100 GeV.

2.2 Finite part

The finite part of the cross section Eq. (4) is defined as

$$Y_f(q_T^2, Q^2, y, \theta, \phi) = \frac{1}{\pi Q^2} \int_{x_A}^1 \frac{dz_A}{z_A} \int_{x_B}^1 \frac{dz_B}{z_B} \sum_{a,b} \sum_{j=1}^{\infty} \left[\frac{\alpha_s(Q)}{2\pi} \right]^j \times R_{ab}^{(j)}(Q^2, z_A, z_B, \theta, \phi) f_{a/A} \left(\frac{x_A}{z_A}, Q \right) f_{b/B} \left(\frac{x_B}{z_B}, Q \right). \quad (26)$$

To order $\mathcal{O}(\alpha_s)$ we only need the function $R^{(1)}$, which is given by the difference of the parts derived from one parton emission, and the pieces which have been removed from the

cross section in the factorization or resummation procedure ($H^{(1)}$ and $\Phi^{(1)}$, respectively). Therefore, we can write

$$R_{ab}^{(1)}(Q^2, z_A, z_B, \theta, \phi) = Q^2 H_{ab}^{(1)}(Q^2, z_A, z_B, \theta, \phi) \delta(s + t + u - Q^2) - \Phi_{ab}^{(1)}(Q^2, z_A, z_B, \theta). \quad (27)$$

$H^{(1)}$ can further be separated into parts which are divergent ($S^{(1)}$) or integrable as $q_T^2 \rightarrow 0$ ($\tilde{H}^{(1)}$), i.e.

$$H_{ab}^{(1)} = \tilde{H}_{ab}^{(1)} + S_{ab}^{(1)}. \quad (28)$$

$S^{(1)}$ can then be combined with $\Phi^{(1)}$ into a function $\Sigma^{(1)}$, so that the whole residue $R^{(1)}$, now in the form

$$R_{ab}^{(1)}(Q^2, z_A, z_B, \theta, \phi) = Q^2 \tilde{H}_{ab}^{(1)}(Q^2, z_A, z_B, \theta, \phi) \delta(s + t + u - Q^2) + \Sigma_{ab}^{(1)}(Q^2, z_A, z_B, \theta), \quad (29)$$

has the property of being integrable as q_T^2 goes to zero. Explicit expressions for functions $\tilde{H}^{(1)}$ and $\Sigma^{(1)}$, as well as the relation of Q^2 , s , t and u to z_A and z_B , are given in Appendix A.

3 Integrated cross section

With our definitions, after integration over q_T , $\cos \theta$ and ϕ , and dropping $\mathcal{O}(\alpha_S^2)$ terms, we recover exactly the order $\mathcal{O}(\alpha_S)$ cross section, which can be written in the form

$$\frac{d\sigma(AB \rightarrow VX)}{dQ^2 dy} = \frac{1}{2^8 N \pi S} \frac{Q^2}{(Q^2 - M_V^2)^2 + M_V^2 \Gamma_V^2} \frac{16}{3} \left[\sum_{a,b}' f'_{a/A}(x_A, Q) f'_{b/B}(x_A, Q) + \frac{\alpha_s(Q)}{2\pi} \int_{x_A}^1 \frac{dz_A}{z_A} \int_{x_B}^1 \frac{dz_B}{z_B} \sum_{a,b} X_{ab}(z_A, z_B) f_{a/A}\left(\frac{x_A}{z_A}, Q\right) f_{b/B}\left(\frac{x_B}{z_B}, Q\right) \right]. \quad (30)$$

In this case the modified parton distribution functions f' are defined as ($a, b \neq g$)

$$f'_{a/A}(x_A, \mu) = \sum_c \int_{x_A}^1 \frac{dz}{z} D_{ac}\left(\frac{x_A}{z}, \mu\right) f_{c/A}(z, \mu), \quad (31)$$

with coefficients

$$D_{ab}(z, \mu) = \delta_{ab} \left\{ \delta(1-z) + \frac{\alpha_S(\mu)}{2\pi} C_F \left[1 - z - \frac{1+z^2}{1-z} \ln\left(\frac{1+z}{2}\right) + (1+z^2) \left(\frac{\ln(1-z)}{1-z} \right)_+ + \left(\frac{\pi^2}{2} - 4 \right) \delta(1-z) \right] \right\}, \quad (32)$$

$$D_{ag}(z, \mu) = \frac{\alpha_S(\mu)}{2\pi} T_R \left[2z(1-z) + [z^2 + (1-z)^2] \ln\left(\frac{2(1-z)}{1+z}\right) \right]. \quad (33)$$

As before, the prime on the sum indicates that gluons are excluded from the summation.

The functions X_{ab} are given as ($X_{\bar{q}q} = X_{q\bar{q}}$, $X_{\bar{q}g} = X_{g\bar{q}}$, $X_{g\bar{q}} = X_{gq}$)

$$X_{\bar{q}q}(z_A, z_B) = G_{\bar{q}q}(z_A, z_B) \left(\frac{1}{(1-z_A)(1-z_B)} \right)_{++} + F_{\bar{q}q}(z_A, z_B), \quad (34)$$

$$X_{qg}(z_A, z_B) = G_{qg}(z_A, z_B) \left(\frac{1}{1-z_A} \right)_+, \quad (35)$$

$$X_{gq}(z_A, z_B) = G_{gq}(z_B, z_A) \left(\frac{1}{1-z_B} \right)_+, \quad (36)$$

where we defined

$$F_{\bar{q}q}(z_A, z_B) = C_F \frac{2(1+z_A z_B)(z_A^2 + z_B^2)}{(z_A + z_B)^2}, \quad (37)$$

$$G_{\bar{q}q}(z_A, z_B) = C_F \frac{2(1+z_A z_B)(z_A^2 + z_B^2)}{(1+z_A)(1+z_B)}, \quad (38)$$

$$G_{qg}(z_A, z_B) = T_R \frac{2z_A(1+z_A z_B)}{(1+z_A)(z_A+z_B)} \left[\frac{(1+z_A z_B)^2 z_B^2}{(z_A+z_B)^2} + (1-z_A z_B)^2 \right]. \quad (39)$$

The definitions of the single and double “plus” distributions used in the above are given in Appendix A. We also remind the reader that results in this section are expressed in terms of \overline{MS} scheme structure functions. Similar expressions in the DIS scheme are presented in Ref. [22].³ Using the techniques of Ref. [22] we can further integrate this to the standard result for the total cross section [23] in the \overline{MS} scheme.

³We believe that the qg contribution in Ref. [22] is in error.

4 Results

As already noted in the introduction, the motivation for this work is that a precise measurement of the W mass at a hadronic collider will depend on accurate theoretical information about its production properties. However, before presenting our results for W and Z production, we would like to address the following issues which in our opinion have not been adequately discussed in the literature: the determination of the form of the non-perturbative function from the low-energy Drell-Yan data, the dependence of the results on the choice of b_{lim} and the matching between low and high q_T .

4.1 Determination of F^{NP}

The unknown function F^{NP} from Eq. (5) has a general form [11]

$$F_{ij}^{NP}(Q, b, x_A, x_B) = \exp \left\{ - \left[h_Q(b) \ln \left(\frac{Q}{2Q_0} \right) + h_i(b, x_A) + h_j(b, x_B) \right] \right\}, \quad (40)$$

where the functions h are not calculable in perturbation theory and therefore must be extracted from experiment. On general grounds, we expect that $h_i \rightarrow 0$ as $b \rightarrow 0$, so that the q_T -integrated cross section is unchanged. On the other hand, the parameter Q_0 is completely arbitrary.

The first attempt to obtain F^{NP} from experiment was made by Davies et al. (DWS) in Ref. [14]. There the functions h were approximated by

$$\begin{aligned} h_Q(b) &= g_2 b^2, \\ h_i(b, x_A) + h_j(b, x_B) &= g_1 b^2, \end{aligned} \quad (41)$$

since the observed q_T distribution at low Q was approximately gaussian in shape. Using the Duke and Owens parton distribution functions [24], DWS determined parameters g_1 and g_2 from E288 [25] data with $\sqrt{S} = 27.4$ GeV, and also from R209 [26] data. The resulting values (with a particular choice of $Q_0 = 2$ GeV) were

$$g_1 = 0.15 \text{ GeV}^2, \quad g_2 = 0.40 \text{ GeV}^2. \quad (42)$$

The cut-off value of b_{lim} from Eq. (18) was chosen to be 0.5 GeV^{-1} . This parameter set yielded a good agreement of theory with R209, as well as with E288 data for $Q < 9 \text{ GeV}$ mass bins. However, for $Q > 11 \text{ GeV}$ theoretical expectations were unacceptably far above the data.

Motivated by the fact that the production of vector bosons at Fermilab Tevatron ($\sqrt{S} = 1.8 \text{ TeV}$) involves values of $\tau = x_A x_B$ which are significantly lower than those considered in Ref. [14], Ladinsky and Yuan (LY) [17] reinvestigated the form of the non-perturbative functions from Eq. (40). Using CTEQ2M parton distribution functions [27], they showed that the DWS form of non-perturbative function (Eqs. (41 and (42)) no longer agrees with R209 data for $5 \text{ GeV} < Q < 8 \text{ GeV}$. In order to improve theoretical predictions, LY postulated the τ dependence for functions h_i , so that

$$\begin{aligned} h_Q(b) &= g_2 b^2, \\ h_i(b, x_A) + h_j(b, x_B) &= g_1 b^2 + g_3 b \ln\left(\frac{\tau}{\tau_0}\right), \end{aligned} \quad (43)$$

where τ_0 is arbitrary parameter.⁴ Choosing $\tau_0 = 0.01$, $Q_0 = 1.6 \text{ GeV}$, and $b_{\text{lim}} = 0.5 \text{ GeV}^{-1}$, these authors determined the non-perturbative parameters by comparison of theory to R209 data [26] in the range $5 \text{ GeV} < Q < 8 \text{ GeV}$, to $\sqrt{S} = 27.4 \text{ GeV}$ E288 data [25] in the range $6 \text{ GeV} < Q < 8 \text{ GeV}$, and also to CDF Z data [28]. In particular, LY explicitly showed that values of

$$g_1 = 0.11_{-0.03}^{+0.04} \text{ GeV}^2, \quad g_2 = 0.58_{-0.2}^{+0.1} \text{ GeV}^2, \quad g_3 = -1.5_{-0.1}^{+0.1} \text{ GeV}^{-1}, \quad (44)$$

provide a good agreement of theory with CDF Z and with R209 data (for $5 \text{ GeV} < Q < 8 \text{ GeV}$), as well as with CDF W data [29]. They furthermore noted that the parameters of Eq. (44) give results which are in agreement with E288 data and with R209 data for $11 \text{ GeV} < Q < 25 \text{ GeV}$.

The problem with using the Drell-Yan data from the fixed-target experiments is that the overall normalization of the cross section is uncertain. For example, the E288 data

⁴We note here that, unlike a simple gaussian, the particular functional form of the non-perturbative function in Eq. (43) is not always positive.

has a stated normalization uncertainty of 25% [25]. Since smearing function F^{NP} simply shifts the q_T distribution between the low and high q_T regions, and since the bulk of the data is in the low q_T region, it is clear that using data with wrong normalization will affect the non-perturbative parameters. Therefore, it is necessary to establish correct normalization for fixed-target experiments before trying to determine the shape of F^{NP} from their data.

A consistent way of determining overall normalization is to compare theoretical predictions for q_T -integrated cross section (to a given order in α_S) with experimental results. We illustrate that procedure for E288 [25] and E605 [30] experiments.⁵

For E288 ($\sqrt{S} = 27.4$ GeV) we used $S d\sigma^2/d\sqrt{\tau}dy$ distributions for the $\sqrt{\tau}$ bins with $Q < 9$ GeV.⁶ In order to achieve agreement with experiment (see Figure 3), we found that theoretical results had to be rescaled down by a factor $K = 0.83 \pm 0.03$.⁷ On the other hand, for the invariant cross section versus q_T data in the range $5 \text{ GeV} < Q < 9 \text{ GeV}$ and $q_T < 2 \text{ GeV}$, the central values of LY parameters yield the best χ^2 of about $7.7/dof$ for $K = 0.75$, while K -factors of 0.80 and 0.83 lead to χ^2 of about $11.9/dof$ and $18.2/dof$, respectively. These results, shown in Figure 4, indicate that parameters of Eq. (44) overestimate the E288 transverse momentum data. We are therefore unconvinced that the parameters of Eq. (44) give the best possible fit to the data.

For E605 ($\sqrt{S} = 38.7$ GeV) we used all available $\sqrt{\tau}$ bins for $S d\sigma^2/d\sqrt{\tau}dy$ distributions, and determined K -factor of $K = 0.88 \pm 0.02$.⁸ The agreement between the theory and the data is illustrated in Figure 5. The corresponding invariant cross section distributions obtained with central values of LY parameters are shown in Figures 6 and 7. From

⁵Unless otherwise stated, all results described in this section are obtained using CTEQ2M parton distribution functions, which facilitates comparison to previous work [17].

⁶The $\sqrt{\tau}$ bins with $Q > 11$ GeV were discarded because of the low statistics.

⁷We define the K -factor as $K = \text{experiment/theory}$. We have chosen to change the normalization of the theory, rather than shifting the experimental data, despite the fact that it is the data which is subject to a normalization uncertainty.

⁸E605 experiment has a stated normalization uncertainty of 15%.

Figure 6 it can be seen that theoretical predictions are in good agreement with experimental results for the bins with $Q < 9$ GeV. However, for bins with $Q > 10.5$ GeV (Figure 7) the theoretical distributions do not match the distributions obtained by experiment.

The LY functional form of F^{NP} given in Eq. (43) implies that theory should be able to describe data with different values of τ . Our results certainly do not support that statement, and we believe that the form of the non-perturbative function remains an open question.

4.2 Choice of b_{lim}

Another issue which has not been addressed in the literature is the dependence of results on the choice of the cut-off value b_{lim} from Eq. (18). In the original work of Ref. [14] b_{lim} was taken to be 0.5 GeV^{-1} because the structure functions were not defined for scales less than 2 GeV. However, this choice is arbitrary. Any change in b_{lim} (in a reasonable range around 0.5 GeV^{-1}) should be compensated by a change in non-perturbative parameters describing F^{NP} , so that an equally good description of experimental data is always achieved.

In order to verify that statement, we attempt to reproduce several different sets of transverse momentum distributions, with b_{lim} chosen in the range from 0.3 GeV^{-1} to 0.7 GeV^{-1} , which one may consider to be reasonable.⁹ We have chosen q_{T} -distributions that include R209 $d\sigma/dq_{\text{T}}^2$ data ($5 \text{ GeV} < Q < 8 \text{ GeV}$, with $q_{\text{T}} < 3 \text{ GeV}$), E288 $Ed\sigma/d^3p$ data for $Q = 5.5, 6.5, 7.5$ and 8.5 GeV (with $q_{\text{T}} < 2 \text{ GeV}$ and K -factor of 0.83), and also E605 $Ed\sigma/d^3p$ data for $Q = 7.5, 8.5, 11$ and 12.5 GeV (with $q_{\text{T}} < 2 \text{ GeV}$ and K -factor of 0.88). Since these data were obtained within a narrow mass range we can neglect the Q -dependence of Eq. (40), and adopt a simple gaussian form for F^{NP} ,

$$F^{NP} = \exp(-g b^2), \quad (45)$$

where g is an effective parameter, different for each of the above q_{T} distributions. In this

⁹Since CTEQ2M structure functions are defined for scales greater than 1.6 GeV, and since $\mu(b) \simeq b_0/b$ for large b , the upper limit of 0.7 GeV^{-1} is still a possible choice for b_{lim} .

way, the task of finding the form of the non-perturbative function is reduced to a simple one-parameter fit. In Figures 8, 9 and 10 we show the best χ^2/dof obtained by varying g with different values of b_{lim} , for R209, E288 and E605 data sets, respectively. It is obvious that for R209 data (where $\sqrt{\tau} = 0.105$) an equally good fit can be obtained regardless of the value chosen for b_{lim} , in part because there is only a small number of data points of limited statistical precision.

However, for E288 and E605 data, which involve larger values of $\sqrt{\tau}$ (for E288 $\sqrt{\tau} = 0.201, 0.238, 0.274$ and 0.311 , while for E605 $\sqrt{\tau} = 0.194, 0.220, 0.284$ and 0.323), the choice of b_{lim} makes a considerable difference, which is not satisfactory from the theoretical point of view. These results might indicate that perhaps a pure gaussian form of the non-perturbative function is wrong.¹⁰ In any case, it is clear that this problem requires a further study.

In Table 1 we also note the range of values for g for which results shown in Figures 8 through 10 were obtained. If the gaussian form of the non-perturbative function were correct, then the values of g , which increase for increasing Q in the E288 and E605 sets, would indicate that the effective coefficient in front of $\ln(Q/(2Q_0))$ in Eq. (40) should be positive, and furthermore that the τ dependence of F^{NP} is not large. However, the values of g obtained for R209 data do not seem to support that observation.

4.3 Matching of low and high q_T regions

The resummation formalism is expected to give a good theoretical description of vector boson production in the low q_T region ($q_T^2 \ll Q^2$). On the other hand, conventional perturbation theory provides a good approximation in the other regime, for $q_T^2 \gg Q^2$. The necessity of matching low and high q_T regions has already been discussed in Ref. [15] for the W and Z production, where it was shown that the proper matching of the pure perturbative and resummed expressions reduces theoretical errors. However, matching

¹⁰There is no reason in principle why the functions h from Eq. (40) should be limited to a quadratic dependence on b .

will never be perfect since resummation introduces higher order terms which will not be cancelled at large q_T in any finite-order calculation of Y_f from Eq. (4). For this reason, the conclusion of Ref. [15] was that one should prefer the ordinary perturbation theory result once the resummed part Y_r becomes negative. For the W and Z production with $\sqrt{S} = 1.8$ TeV this happens at $q_T \sim 50$ GeV. In Ref. [15] it was also shown that matching works well with the second-order calculation of Y_f . For example, at q_T of about 50 GeV the mismatch between the q_T distribution calculated using resummation plus the $\mathcal{O}(\alpha_S^2)$ calculation of Y_f and the one calculated using conventional second-order perturbation theory was of the order of 10%.

In Figure 11 we show our results for the W production, obtained with gaussian and LY form of F^{NP} , compared to the $\mathcal{O}(\alpha_S)$ perturbative result. At q_T of 50 GeV the mismatch between Y_r plus the $\mathcal{O}(\alpha_S)$ calculation of Y_f and perturbation theory is about 50%. For the γ^* production at fixed target experiments the same problem (but even more acute) is illustrated in Figure 12 for E288 experiment (with $5 \text{ GeV} < Q < 6 \text{ GeV}$ and $-0.27 < y < 0.33$). These two figures clearly indicate the necessity for extending the results of Ref. [15] to include the decay of the vector boson, if a complete theoretical description is desired. Nevertheless, we emphasize that results presented in this paper are obtained for the low q_T region, where the resummation formalism plus the $\mathcal{O}(\alpha_S)$ calculation of Y_f should be adequate. Note also that it is the region of low q_T which is of interest for the W mass measurement.

4.4 Results for the W and Z production

Once the high statistics data on the vector boson q_T distributions at 1.8 TeV become available, one can extract the effective form of F^{NP} from the Z data, and use that information to obtain an accurate theoretical prediction for the various q_T -dependent distributions of the W boson.¹¹ This in turn should allow a precise measurement of the

¹¹Taking current values of vector boson masses [31], at $\sqrt{S} = 1.8$ TeV for $Q = M_W(M_Z)$ the value of $\sqrt{\tau}$ is about 0.045(0.051).

W mass.

For the data available at present [28, 29] the statistics is low, which limits the predictive power of the resummation formalism. In order to illustrate that, we again adopt a simple parametrization of F^{NP} given in Eq. (45), choose $b_{\text{lim}} = 0.5 \text{ GeV}^{-1}$, and vary g in an attempt to obtain a good fit to the $W = W^+ + W^-$ and Z $d\sigma/dq_T$ data.¹² As shown in Figure 13, due to large statistical errors almost any choice of g in the range between of about 1.5 GeV^2 to about 5 GeV^2 yields an acceptable description of both data sets. We conclude that it does not make much sense to use these data for determination of F^{NP} , and that data with much higher statistics are needed before any firm theoretical predictions can be made for the W and Z production. Nevertheless, we still observe that the effective value for g obtained from the Z data tends to be smaller than the one obtained from the W data. This is in disaccord with what one would expect from the fixed target data (see Table 1), and may again indicate that pure gaussian form for F^{NP} is not correct. It may also indicate experimental biases introduced by the selection of two isolated leptons in the Z sample.

In Figures 14 and 15 we show our results for the W and Z q_T distributions. These results are obtained with F^{NP} given in Eq. (45), with $g = 3.0 \text{ GeV}^2$ and $b_{\text{lim}} = 0.5 \text{ GeV}^{-1}$, using several different parton distribution functions. Besides illustrating the α_S dependence of $d\sigma/dq_T$,¹³ these two figures also show that the fit to the data is as good as the one obtained in Ref. [17], even though we used much simpler functional form of F^{NP} .

We now consider briefly the import of these results for the measurement of the W mass. Figure 16 shows the transverse mass m_T of the lepton pair, obtained with the two different choices of F^{NP} . To first order the transverse mass is insensitive to the transverse motion of the W , and because of that the m_T distribution is largely independent of the non-perturbative parameters.

¹²We assumed $BR(Z \rightarrow e^+e^-) = 0.033$ and $BR(W^+ \rightarrow e^+\nu) = 0.111$, as was done in [28] and [29], respectively.

¹³For CTEQ2M [27], MRSR1 and MRSR2 [32], we used $\alpha_S(M_Z)$ of 0.110, 0.113 and 0.120, respectively.

As the luminosity of the Tevatron is increased the number of interactions per beam crossing will increase, leading to a degradation of the missing energy resolution. Therefore the measurement of the Jacobian peak in the lepton transverse momentum will become a competitive method of measuring the W mass. Figure 17 shows the expected transverse momentum distribution of the electron from W^- decay. The width of this distribution is broader than the transverse mass distribution and the dependence on the non-perturbative functions is larger. A quantitative estimate of the size of this dependence will have to await a reliable extraction of the non-perturbative parameters.

5 Conclusions

In view of the large number of W and Z bosons to be expected in Run II at the Tevatron we have returned to consider their production and decay in hadronic collisions. We have provided a description of vector boson production which not only gives a correct description at small q_T , but also reproduces the correct formula for the q_T -integrated cross section. In addition we have included the decay of the vector bosons so that experimental cuts can be included.

In the course of our numerical work we have raised several issues which have not been adequately addressed in the literature. The analysis of the low energy experiments needs to be repeated, using the q_T -integrated data to fix the overall normalization, before any attempt to determine the form of the non-perturbative function is made. Furthermore, this analysis should include all low energy experiments for which q_T -dependent distributions are available. On the other hand, for the W mass measurement the effective form of the non-perturbative function can be extracted from the Z data. This would eliminate uncertainties related to the determination of F^{NP} from the low energy experiments.

Besides the form of the non-perturbative function, there are also other theoretical problems which have to be resolved. In particular, we have shown the necessity for extending the results of Ref. [15] to include the vector boson decay, if a more complete

theoretical description of the leptons coming from that decay is desired. As shown in Ref. [15], for the W and Z production at Tevatron the $\mathcal{O}(\alpha_S^2)$ calculation of the finite part of Eq. (4) should yield satisfactory results for matching of low and high transverse momentum regions. However, it is not quite clear whether such a calculation would entirely solve the problem of getting a complete description of the q_T distribution for the γ^* production in the low energy experiments.

ACKNOWLEDGMENTS

This work was supported in part by the U.S. Department of Energy under Contracts No. DE-AC02-76CH03000. R.K.E. and D.A.R. thank the CERN theory group for hospitality.

A Details of the formulae

A.1 Couplings

In this appendix we document the results for functions $H^{(0)}$, $H^{(1)}$, and $\Sigma^{(1)}$ which appear in Eqs. (11) and (29). These functions can all be separated into parts which are even and odd under parity, e.g. we can write $H^{(0)} = H^{(0)+} + H^{(0)-}$. Consequently, we first define “plus” and “minus” quark-quark and quark-gluon couplings as

$$\mathcal{V}_{qq'}^+ = |V_{qq'}|^2 (g_L^2 + g_R^2) (f_L^2 + f_R^2) , \quad (46)$$

$$\mathcal{V}_{qq'}^- = |V_{qq'}|^2 (g_L^2 - g_R^2) (f_L^2 - f_R^2) , \quad (47)$$

and

$$\mathcal{V}_{qg}^+ = \sum_{q'} |V_{qq'}|^2 (g_L^2 + g_R^2) (f_L^2 + f_R^2) , \quad (48)$$

$$\mathcal{V}_{qg}^- = \sum_{q'} |V_{qq'}|^2 (g_L^2 - g_R^2) (f_L^2 - f_R^2) , \quad (49)$$

where g_L , g_R , f_L and f_R are listed in Table 2. The coefficients $V_{qq'}$ are elements of the Cabibbo-Kobayashi-Maskawa matrix for the W production, and are equal to $\delta_{qq'}$ in the case of Z or massive photon γ^* .

In the case of l^+l^- production, which can proceed through the exchange of either a Z or a γ^* , the above expressions need to be modified by making the replacements ($Q_e = -1$, $Q_u = 2/3$, and $Q_d = -1/3$)

$$\begin{aligned} (g_L^2 + g_R^2)(f_L^2 + f_R^2) &\rightarrow (g_L^2 + g_R^2)(f_L^2 + f_R^2) + 4e^4 Q_f^2 Q_e^2 \chi_2(Q^2) \\ &+ 2e^2 Q_f Q_e (g_L f_L + g_R f_R + g_L f_R + g_R f_L) \chi_1(Q^2), \end{aligned} \quad (50)$$

$$\begin{aligned} (g_L^2 - g_R^2)(f_L^2 - f_R^2) &\rightarrow (g_L^2 - g_R^2)(f_L^2 - f_R^2) \\ &+ 2e^2 Q_f Q_e (g_L f_L + g_R f_R - g_L f_R - g_R f_L) \chi_1(Q^2), \end{aligned} \quad (51)$$

with

$$\chi_1(Q^2) = \frac{(Q^2 - M_Z^2)}{Q^2}, \quad (52)$$

$$\chi_2(Q^2) = \frac{(Q^2 - M_Z^2)^2 + M_Z^2 \Gamma_Z^2}{Q^4}. \quad (53)$$

In these expressions e^2 is the electromagnetic charge which is taken to run (down from its value at the Z coupling) using the one loop electromagnetic β function,

$$\frac{d\alpha}{d \ln Q^2} = \frac{\alpha^2}{3\pi} \left[\sum_l + 3 \sum_f Q_f^2 \right]. \quad (54)$$

At $Q = 5$ GeV we find that $\alpha \simeq 1/133$.

In our numerical work we choose four input parameters¹⁴

$$G_F = 1.16639 \times 10^{-5} \text{ GeV}^{-2},$$

¹⁴The boson widths are fixed at their measured values

$$\Gamma_W = 2.07 \text{ GeV}, \quad \Gamma_Z = 2.49 \text{ GeV}.$$

These, as well as all other parameters, are taken from the Review of Particle Properties [31].

$$\begin{aligned}
M_Z &= 91.187 \text{ GeV} , \\
\alpha(M_Z) &= (128.89)^{-1} , \\
M_W &= 80.33 \text{ GeV} .
\end{aligned} \tag{55}$$

In terms of these parameters we can derive the ρ parameter

$$\rho = \frac{M_W^2}{M_Z^2} \left[1 - \frac{\pi\alpha(M_Z)}{\sqrt{2}G_F M_W^2} \right]^{-1} = 1.00654 , \tag{56}$$

which enters in the couplings (see Table 2) in the improved Born approximation:

$$\begin{aligned}
g_W^2 &= 4\sqrt{2}M_W^2 G_F , \\
g_Z^2 &= \sqrt{2}G_F M_Z^2 \rho , \\
x_W &= 1 - \frac{M_W^2}{\rho M_Z^2} .
\end{aligned} \tag{57}$$

A.2 Matrix elements

We start by considering the lowest order process for the production of a vector boson of mass M_V and width Γ_V (the momenta are shown in brackets),

$$q(p_1) + \bar{q}(p_2) \rightarrow l(k_1) + \bar{l}(k_2) . \tag{58}$$

The matrix element squared for lowest order process averaged (summed) over the initial (final) spins and colours ($N = 3$) is given by

$$\overline{\sum} |M_{q\bar{q}}|^2 = \frac{1}{4N} \frac{Q^4}{(Q^2 - M_V^2)^2 + M_V^2 \Gamma_V^2} H_{q\bar{q}}^{(0)} , \tag{59}$$

where

$$H_{q\bar{q}}^{(0)} = \frac{8}{Q^4} \left[\mathcal{V}_{q\bar{q}}^+ (p_1 \cdot k_2 p_2 \cdot k_1 + p_1 \cdot k_1 p_2 \cdot k_2) + \mathcal{V}_{q\bar{q}}^- (p_1 \cdot k_2 p_2 \cdot k_1 - p_1 \cdot k_1 p_2 \cdot k_2) \right] . \tag{60}$$

It is convenient to express the above matrix element in terms of angular variables in the Collins-Soper (CS) frame, which is defined by

$$\begin{aligned}
k_1^\mu &= \frac{Q}{2} (1, \sin \phi \sin \theta, \cos \phi \sin \theta, \cos \theta) , \\
k_2^\mu &= \frac{Q}{2} (1, -\sin \phi \sin \theta, -\cos \phi \sin \theta, -\cos \theta) , \\
p_1^\mu &= -\frac{(t - Q^2)}{2Q} (1, 0, -\sin \beta, \cos \beta) , \\
p_2^\mu &= -\frac{(u - Q^2)}{2Q} (1, 0, -\sin \beta, -\cos \beta) ,
\end{aligned} \tag{61}$$

with¹⁵

$$\tan \beta = \frac{q_T}{Q} . \tag{62}$$

In the terms of the vector boson transverse momentum ($q_T = |\mathbf{q}_T|$) and rapidity (y) in the lab frame, we also have

$$q^\mu = (M_T \cosh y, \mathbf{q}_T, M_T \sinh y) , \tag{63}$$

where $M_T^2 = Q^2 + q_T^2$ and $Q^2 = q^2$. We further define several functions which determine the angular dependence as

$$\begin{aligned}
\mathcal{L}_0 &= 1 + \cos^2 \theta , \\
\mathcal{A}_0 &= \frac{1}{2}(1 - 3 \cos^2 \theta) , \\
\mathcal{A}_1 &= \sin 2\theta \cos \phi , \\
\mathcal{A}_2 &= \frac{1}{2} \sin^2 \theta \cos 2\phi , \\
\mathcal{A}_3 &= 2 \cos \theta , \\
\mathcal{A}_4 &= \sin \theta \cos \phi .
\end{aligned} \tag{64}$$

Using these angular variables Eq. (60) may be written as,

$$H_{q\bar{q}}^{(0)}(\theta) = \mathcal{V}_{q\bar{q}}^+ \mathcal{L}_0 + \mathcal{V}_{q\bar{q}}^- \mathcal{A}_3 . \tag{65}$$

¹⁵In lowest order the vector boson is produced at zero transverse momentum and hence $\beta = 0$.

Note the relation between the $q\bar{q}$ and $\bar{q}q$ processes,

$$H_{q\bar{q}}^{(0)}(\theta) = H_{\bar{q}q}^{(0)}(\pi - \theta) . \quad (66)$$

We next consider $\tilde{H}^{(1)}$ and $\Sigma^{(1)}$ (needed for the finite part of Eq. (4)), which are derived from the matrix element squared for processes involving one parton emission, and from the pieces removed from the cross section in the resummation procedure, (*cf.* Eqs. (28) and (29)). It is sufficient to calculate results for the two-to-three processes

$$q(p_1) + \bar{q}(p_2) \rightarrow l(k_1) + \bar{l}(k_2) + g(k_3) , \quad (67)$$

$$q(p_1) + g(p_2) \rightarrow l(k_1) + \bar{l}(k_2) + q'(k_3) , \quad (68)$$

as all other processes are determined by the crossing relations. The invariant variables for the above processes are

$$\begin{aligned} s &= (p_1 + p_2)^2 , \\ q^2 &= Q^2 = (k_1 + k_2)^2 , \\ t &= (p_1 - q)^2 = (p_2 - k_3)^2 , \\ u &= (p_2 - q)^2 = (p - k_3)^2 . \end{aligned} \quad (69)$$

The matrix element squared can be put in the form

$$\overline{\sum} |M_{ab}|^2 = \frac{g^2}{2N} \frac{Q^2}{(Q^2 - M_V^2)^2 + M_V^2 \Gamma_V^2} H_{ab}^{(1)} , \quad (70)$$

with

$$\begin{aligned} H_{q\bar{q}}^{(1)} &= \frac{8C_F}{tu} \left\{ \mathcal{V}_{q\bar{q}}^+ \left[(p_2 \cdot k_1)^2 + (p_1 \cdot k_2)^2 + (p_2 \cdot k_2)^2 + (p_1 \cdot k_1)^2 \right] \right. \\ &\quad \left. + \mathcal{V}_{q\bar{q}}^- \left[(p_2 \cdot k_1)^2 + (p_1 \cdot k_2)^2 - (p_2 \cdot k_2)^2 - (p_1 \cdot k_1)^2 \right] \right\} , \end{aligned} \quad (71)$$

$$\begin{aligned} H_{qg}^{(1)} &= -\frac{8T_R}{ts} \left\{ \mathcal{V}_{qg}^+ \left[(k_3 \cdot k_1)^2 + (p_1 \cdot k_2)^2 + (k_3 \cdot k_2)^2 + (p_1 \cdot k_1)^2 \right] \right. \\ &\quad \left. + \mathcal{V}_{qg}^- \left[(k_3 \cdot k_1)^2 + (p_1 \cdot k_2)^2 - (k_3 \cdot k_2)^2 - (p_1 \cdot k_1)^2 \right] \right\} . \end{aligned} \quad (72)$$

Again, using Eq. (61) the functions $H^{(1)}$ can be expressed in terms of invariant variables and the angles in the CS frame

$$H_{ab}^{(1)} \rightarrow H_{ab}^{(1)}(Q^2, t, u, \theta, \phi) . \quad (73)$$

Before writing down the expressions for $\tilde{H}^{(1)}$ and $\Sigma^{(1)}$, we clarify the relationship between different variables. The Mandelstam variables for the parton subprocess can be expressed in terms of the integration variables in Eq. (26) ($z_A = x_A/\xi_A$ and $z_B = x_B/\xi_B$) as

$$\begin{aligned} s &= \frac{Q^2}{z_A z_B} , \\ t &= -\frac{Q^2}{z_A}(\eta - z_A) , \\ u &= -\frac{Q^2}{z_B}(\eta - z_B) , \end{aligned} \quad (74)$$

where $M_T = \sqrt{Q^2 + q_T^2}$ and $\eta = M_T/Q$. We further note that if $Q^2 = s + t + u$ and $q_T^2 = ut/s$ one can derive

$$\eta = \frac{M_T}{Q} \equiv \frac{1 + z_A z_B}{z_A + z_B} , \quad (75)$$

so that $Q^2 (\equiv q_T^2/(\eta^2 - 1))$ can be expressed in terms of q_T^2 , z_A and z_B .

For the process $q\bar{q} \rightarrow \bar{l}l g$ we have $\tilde{H}_{q\bar{q}}^{(1)} = \tilde{H}_{q\bar{q}}^{(1)+} + \tilde{H}_{q\bar{q}}^{(1)-}$, with¹⁶

$$\tilde{H}_{q\bar{q}}^{(1)+}(Q^2, t, u, \theta, \phi) = \mathcal{V}_{q\bar{q}}^+ \frac{C_F}{s} \left\{ \mathcal{R}_+(t, u) \frac{1}{M_T^2} (\mathcal{L}_0 + \mathcal{A}_0 + \mathcal{A}_2) - \mathcal{R}_-(t, u) \frac{Q}{q_T M_T^2} \mathcal{A}_1 \right\} , \quad (76)$$

$$\tilde{H}_{q\bar{q}}^{(1)-}(Q^2, t, u, \theta, \phi) = \mathcal{V}_{q\bar{q}}^- \frac{C_F}{s} \left\{ \mathcal{R}_+(t, u) \frac{Q}{q_T^2 M_T} \left(1 - \frac{Q}{M_T}\right) \mathcal{A}_3 - \mathcal{R}_-(t, u) \frac{2}{q_T M_T} \mathcal{A}_4 \right\} . \quad (77)$$

Here,

$$\mathcal{R}_{\pm}(t, u) = (Q^2 - t)^2 \pm (Q^2 - u)^2 . \quad (78)$$

¹⁶The term proportional to \mathcal{A}_1 in Eq. (76) differs from the analogous expression in Eq. (16) of Ref. [19]. In addition, Eqs. (16)-(18) of Ref. [19] are missing colour factors.

Similarly, for $qg \rightarrow l\bar{l}q'$ ($\tilde{H}_{qg}^{(1)} = \tilde{H}_{qg}^{(1)+} + \tilde{H}_{qg}^{(1)-}$) we have

$$\begin{aligned} \tilde{H}_{qg}^{(1)+}(Q^2, t, u, \theta, \phi) &= -\mathcal{V}_{qg}^+ \frac{T_R}{st} \left\{ (\mathcal{R}_+(t, s) - \mathcal{R}_+(0, s)) \mathcal{L}_0 + \frac{q_T^2}{M_T^2} \left[\mathcal{R}_+(t, -s) (\mathcal{A}_0 + \mathcal{A}_2) \right. \right. \\ &\quad \left. \left. - \left((Q^2 - t)^2 + \mathcal{R}_-(t, u) \right) \frac{Q}{q_T} \mathcal{A}_1 \right] \right\}, \end{aligned} \quad (79)$$

$$\begin{aligned} \tilde{H}_{qg}^{(1)-}(Q^2, t, u, \theta, \phi) &= -\mathcal{V}_{qg}^- \frac{T_R}{st} \left\{ \left(\frac{Q}{M_T} \mathcal{R}_+(t, s) - \mathcal{R}_+(0, s) - 2 \frac{Q}{M_T} t(Q^2 - s) \right) \mathcal{A}_3 \right. \\ &\quad \left. - \frac{2q_T}{M_T} \left[2s(Q^2 - s) + \mathcal{R}_+(t, s) \right] \mathcal{A}_4 \right\}. \end{aligned} \quad (80)$$

Note that the crossing relationships for all other two-to-three processes are given as

$$\begin{aligned} \tilde{H}_{q\bar{q}}^{(1)}(Q^2, t, u, \theta, \phi) &= \tilde{H}_{q\bar{q}}^{(1)}(Q^2, u, t, \pi - \theta, \phi), \\ \tilde{H}_{gq}^{(1)}(Q^2, t, u, \theta, \phi) &= \tilde{H}_{gq}^{(1)}(Q^2, u, t, \pi - \theta, \phi), \\ \tilde{H}_{q\bar{g}}^{(1)}(Q^2, t, u, \theta, \phi) &= \tilde{H}_{q\bar{g}}^{(1)}(Q^2, t, u, \pi - \theta, \pi - \phi), \\ \tilde{H}_{g\bar{q}}^{(1)}(Q^2, t, u, \theta, \phi) &= \tilde{H}_{g\bar{q}}^{(1)}(Q^2, u, t, \theta, \pi - \phi). \end{aligned} \quad (81)$$

The corresponding expressions for $\Sigma_{q\bar{q}}^{(1)}$ and $\Sigma_{qg}^{(1)}$ look simpler when written in terms of z_A and z_B ,

$$\Sigma_{q\bar{q}}^{(1)}(Q^2, z_A, z_B, \theta) = r_{q\bar{q}}(Q^2, z_A, z_B) \frac{Q^2}{q_T^2} (\mathcal{V}_{q\bar{q}}^+ \mathcal{L}_0 + \mathcal{V}_{q\bar{q}}^- \mathcal{A}_3), \quad (82)$$

$$\Sigma_{qg}^{(1)}(Q^2, z_A, z_B, \theta) = r_{qg}(Q^2, z_A, z_B) \frac{Q^2}{q_T^2} (\mathcal{V}_{qg}^+ \mathcal{L}_0 + \mathcal{V}_{qg}^- \mathcal{A}_3). \quad (83)$$

Here, the functions r are given as

$$\begin{aligned} r_{q\bar{q}}(Q^2, z_A, z_B) &= C_F \left\{ (z_A^2 + z_B^2) \delta(1 - \eta z_A - \eta z_B + z_A z_B) \right. \\ &\quad - \Theta(Q^2 - q_T^2) \delta(1 - z_B) \left(\frac{1 + z_A^2}{1 - z_A} \right)_+ - \Theta(Q^2 - q_T^2) \delta(1 - z_A) \left(\frac{1 + z_B^2}{1 - z_B} \right)_+ \\ &\quad \left. - 2\Theta(Q^2 - q_T^2) \delta(1 - z_A) \delta(1 - z_B) \left[\ln \left(\frac{Q^2}{q_T^2} \right) - \frac{3}{2} \right] \right\}, \end{aligned} \quad (84)$$

and

$$r_{qg}(Q^2, z_A, z_B) = T_R \left\{ z_A(\eta - z_B) \left[z_A^2 z_B^2 + (1 - z_A z_B)^2 \right] \delta(1 - \eta z_A - \eta z_B + z_A z_B) \right. \\ \left. - \Theta(Q^2 - q_T^2) \left[z_B^2 + (1 - z_B)^2 \right] \delta(1 - z_A) \right\}. \quad (85)$$

When using crossing relationships analogous to Eq. (81) for $\Sigma^{(1)}$ one should remember that $t \leftrightarrow u$ implies $z_A \leftrightarrow z_B$.

From Eqs. (77)-(80) it is evident that $\tilde{H}^{(1)}$ is an integrable function of q_T^2 at $q_T^2 \rightarrow 0$. We now show this is also true of Eqs. (82) and (83). Define

$$x_A^* = \frac{1 - \eta x_B}{\eta - x_B}, \quad x_B^* = \frac{1 - \eta x_A}{\eta - x_A}, \quad (86)$$

and consider the integral J_{ab}

$$J_{ab} = \int_{x_A}^1 \frac{dz_A}{z_A} \int_{x_B}^1 \frac{dz_B}{z_B} f_a\left(\frac{x_A}{z_A}\right) f_b\left(\frac{x_B}{z_B}\right) r_{ab}(Q^2, z_A, z_B). \quad (87)$$

Inserting the explicit form of $r_{q\bar{q}}$ from Eq. (84) and using the representation

$$\ln \frac{q_T^2}{Q^2} \equiv \ln[\eta^2 - 1] = \ln[(\eta - x_A)(\eta - x_B)] - \int_{x_A}^{x_A^*} \frac{dz_A}{\eta - z_A}, \quad (88)$$

we find

$$J_{q\bar{q}} = \int_{x_A}^1 dz_A \int_{x_B}^1 dz_B \delta(1 - \eta z_A - \eta z_B + z_A z_B) \\ \times \left[g_{q\bar{q}}(z_A, z_B) - g_{q\bar{q}}(z_A, 1) - g_{q\bar{q}}(1, z_B) + g_{q\bar{q}}(1, 1) \right] \\ + \int_{x_A}^1 dz_A \left[g_{q\bar{q}}(z_A, 1) - g_{q\bar{q}}(1, 1) \right] \left[\frac{\Theta(x_A^* - z_A)}{(\eta - z_A)} - \frac{\Theta(Q^2 - q_T^2)}{(1 - z_A)} \right] \\ + \int_{x_B}^1 dz_B \left[g_{q\bar{q}}(1, z_B) - g_{q\bar{q}}(1, 1) \right] \left[\frac{\Theta(x_B^* - z_B)}{(\eta - z_B)} - \frac{\Theta(Q^2 - q_T^2)}{(1 - z_B)} \right] \\ + g_{q\bar{q}}(1, 1) \left[\ln \left(\frac{(\eta - x_A)(\eta - x_B)}{(1 - x_A)(1 - x_B)} \right) + \Theta(q_T^2 - Q^2) \ln \left(\frac{(1 - x_A)(1 - x_B)}{\eta^2 - 1} \right) \right], \quad (89)$$

with

$$g_{q\bar{q}}(z_A, z_B) = C_F \frac{z_A^2 + z_B^2}{z_A z_B} f_q\left(\frac{x_A}{z_A}\right) f_{\bar{q}}\left(\frac{x_B}{z_B}\right). \quad (90)$$

In this form the vanishing of $J_{q\bar{q}}$ in the limit $\eta \rightarrow 1$ is manifest. Similarly, using Eq. (85) for r_{qg} we obtain

$$J_{qg} = \int_{x_B}^1 dz_B \left[g_{qg}(z_A^*, z_B) \Theta(x_B^* - z_B) - \Theta(Q^2 - q_T^2) g_{qg}(1, z_B) \right], \quad (91)$$

where $z_A^* = (1 - \eta z_B)/(\eta - z_B)$ and

$$g_{qg}(z_A, z_B) = T_R \frac{z_A^2 z_B^2 + (1 - z_A z_B)^2}{z_B} f_q\left(\frac{x_A}{z_A}\right) f_g\left(\frac{x_B}{z_B}\right). \quad (92)$$

Clearly, in the limit $\eta \rightarrow 1$ we have that $J_{qg} \rightarrow 0$.

A.3 “Plus” distributions

The definition of single plus distribution used in Section 3 and in this appendix is the standard one,

$$\int_x^1 dz f(z) [g(z)]_+ = \int_x^1 dz [f(z) - f(1)] g(z) - f(1) \int_0^x dz g(z). \quad (93)$$

In Section 3 we also used the double plus distribution defined as

$$\begin{aligned} & \int_{x_A}^1 dz_A \int_{x_B}^1 dz_B f(z_A, z_B) \left(\frac{1}{(1 - z_A)(1 - z_B)} \right)_{++} = \\ & = \int_{x_A}^1 dz_A \int_{x_B}^1 dz_B \frac{f(z_A, z_B) - f(z_A, 1) - f(1, z_B) + f(1, 1)}{(1 - z_A)(1 - z_B)} \\ & + \int_{x_A}^1 dz_A f(z_A, 1) \left(\frac{1}{1 - z_A} \right)_+ \ln(1 - x_B) + \int_{x_B}^1 dz_B f(1, z_B) \left(\frac{1}{1 - z_B} \right)_+ \ln(1 - x_A) \\ & - f(1, 1) \ln(1 - x_A) \ln(1 - x_B). \end{aligned} \quad (94)$$

B Numerical evaluation of Bessel transform

When q and b become large it is convenient to use the asymptotic expansion¹⁷ to evaluate that portion of the Bessel transform because of the large cancellations between different

¹⁷This method was suggested in [15]. The formula corresponding to Eq. (95) in Ref. [15] contains an overall sign error.

cycles of the Bessel function. For large b we find that

$$\int_b^\infty dy J_0(qy)h(y) = \sqrt{\frac{2}{\pi q}} \sum_{n=0}^\infty \frac{1}{q^{n+1}} \sum_{k=0}^n \frac{\Gamma(\frac{1}{2} + k)}{2^k k! \Gamma(\frac{1}{2} - k)} \times \cos\left(qb + n\frac{\pi}{2} + \frac{\pi}{4}\right) \frac{d^{(n-k)}}{d^{(n-k)}b} \left[\frac{h(b)}{b^{k+\frac{1}{2}}} \right]. \quad (95)$$

If we further make the special choice of $b = b_s$

$$b_s = \left(2s + \frac{1}{4}\right) \frac{\pi}{q}, \quad s = 1, 2, 3, \dots, \quad (96)$$

the even n terms will cancel because

$$\cos\left(qb_s + n\frac{\pi}{2} + \frac{\pi}{4}\right) = -\sin\left(n\frac{\pi}{2}\right), \quad (97)$$

and we have

$$\int_{b_s}^\infty dy J_0(qy)h(y) = -\frac{1}{q} \sqrt{\frac{2}{\pi}} \frac{1}{(qb_s)^{\frac{3}{2}}} \left\{ \left[b_s h'(b_s) - \frac{5}{8} h(b_s) \right] + O\left(\frac{1}{(qb_s)^2}\right) \right\}. \quad (98)$$

In practice it is found that the explicit integration needs to be done over only a few cycles, before approximating with the asymptotic expansion, Eq. (98).

References

- [1] H. Fritzsche and P. Minkowski, *Phys. Lett.* **B73**, 80 (1978);
G. Altarelli, G. Parisi and R. Petronzio, *Phys. Lett.* **B76**, 351 (1978);
K. Kajantie and R. Raitio, *Nucl. Phys.* **B139**, 72 (1978);
F. Halzen and D.M. Scott, *Phys. Rev.* **D18**, 3379 (1978).
- [2] R.K. Ellis, G. Martinelli and R. Petronzio, *Nucl. Phys.* **B211**, 106 (1983).
- [3] P. Arnold and M.H. Reno, *Nucl. Phys.* **B319**, 37 (1989), Erratum *Nucl. Phys.* **B330**, 284 (1990);
P. Arnold, R.K. Ellis and M.H. Reno, *Phys. Rev.* **D40**, 912 (1989).
- [4] R. Gonsalves, J. Pawlowski and C-F Wai, *Phys. Rev.* **D40**, 2245 (1989).
- [5] P. Aurenche and J. Lindfors, *Phys. Lett.* **B96**, 171 (1980).
- [6] E. Mirkes, *Nucl. Phys.* **B387**, 3 (1992);
E. Mirkes and J. Ohnemus, *Phys. Rev.* **D51**, 4891 (1995).
- [7] W. Giele, E. Glover, D.A. Kosower, *Nucl. Phys.* **B403**, 633 (1993),
Phys. Lett. **B309**, 205 (1993).
- [8] Yu.L. Dokshitzer, D.I. Dyakonov and S.I. Troyan, *Phys. Rep.* **58**, 269 (1980).
- [9] G. Parisi and R. Petronzio, *Nucl. Phys.* **B154**, 427 (1979).
- [10] C. Davies and W.J. Stirling, *Nucl. Phys.* **B244**, 337 (1984).
- [11] J. Collins, D. Soper and G. Sterman, *Nucl. Phys.* **B250**, 199 (1985).
- [12] J.C. Collins and D. Soper, *Nucl. Phys.* **B193**, 381 (1981); Erratum *Nucl. Phys.* **B213**, 545 (1983); *Nucl. Phys.* **B197**, 446 (1982).
- [13] G. Altarelli, R.K. Ellis, M. Greco, G. Martinelli, *Nucl. Phys.* **B246**, 12 (1984).

- [14] C. Davies, B.R. Webber and W.J. Stirling, *Nucl. Phys.* **B256**, 413 (1985).
- [15] P.B. Arnold and R.P. Kauffman, *Nucl. Phys.* **B349**, 381 (1991).
- [16] H. Baer and M.H. Reno, *Phys. Rev.* **D47**, 3906 (1993); *Phys. Rev.* **D43**, 2892 (1990); *Phys. Rev.* **D45**, 1503 (1992).
- [17] G.A. Ladinsky and C.-P. Yuan, *Phys. Rev.* **D50**, 4239 (1994).
- [18] M.H. Reno, *Phys. Rev.* **D49**, 4326 (1994).
- [19] C. Balázs, J. Qiu, and C.-P. Yuan, *Phys. Lett.* **B355**, 548 (1995).
- [20] J. Collins and D. Soper, *Phys. Rev.* **D16**, 2219 (1977).
- [21] C.T.H. Davies, University of Cambridge Ph.D. thesis, (1984).
- [22] J. Kubar *et al.*, *Nucl. Phys.* **B175**, 251 (1980).
- [23] For a review see, R.K. Ellis, W.J. Stirling and B.R. Webber, *QCD and Collider Physics*, Cambridge University Press, (1996).
- [24] D.W. Duke and J.F. Owens, *Phys. Rev.* **D30**, 49 (1984).
- [25] A.S. Ito *et al.*, *Phys. Rev.* **D23**, 604 (1981).
- [26] D. Antreasyan *et al.*, *Phys. Rev. Lett.* **47**, 12 (1981), *ibid.* **48**, 302 (1982).
- [27] CTEQ2 structure functions, see Wu-Ki Tung, *Proceedings of the Workshop on Deep Inelastic Scattering and related subjects*, Eilat, Israel, Ed. A. Levy, World Scientific, (1994).
- [28] F. Abe *et al.*, *Phys. Rev. Lett.* **67**, 2937 (1991).
- [29] F. Abe *et al.*, *Phys. Rev. Lett.* **66**, 2951 (1991).

- [30] G. Moreno *et al.*, *Phys. Rev.* **D43**, 2815 (1991).
- [31] R.M. Barnett *et al.*, *Phys. Rev.* **D54**, 1 (1996).
- [32] A.D. Martin, R.G. Roberts and W.J. Stirling, *Phys. Lett.* **B387**, 419 (1996).

Table 1: The range of values for g for which results shown in Figures 8 through 10 were obtained.

Experiment	Range in Q [GeV]	Range in $\sqrt{\tau}$	Range in g [GeV ²]
R209	5 – 8	0.081 – 0.129	0.52 – 0.55
E288	5 – 6	0.182 – 0.219	0.30 – 0.35
	6 – 7	0.219 – 0.255	0.32 – 0.40
	7 – 8	0.255 – 0.292	0.33 – 0.46
	8 – 9	0.292 – 0.328	0.38 – 0.50
E605	7 – 8	0.180 – 0.206	0.34 – 0.41
	8 – 9	0.206 – 0.232	0.42 – 0.49
	10.5 – 11.5	0.271 – 0.296	0.46 – 0.53
	11.5 – 13.5	0.296 – 0.348	0.46 – 0.51

Table 2: Vector boson couplings in the notation given in the Appendix A. Lepton and quark charges are $Q_e = -1$, $Q_u = 2/3$, and $Q_d = -1/3$.

Boson	f_L	f_R	g_L	g_R
W	$g_W/\sqrt{2}$	0	$g_W/\sqrt{2}$	0
Z	$g_Z(T_3 - Q_e x_W)$	$-g_Z Q_e x_W$	$g_Z(T_3 - Q_f x_W)$	$-g_Z Q_f x_W$
γ^*	eQ_e	eQ_e	eQ_f	eQ_f

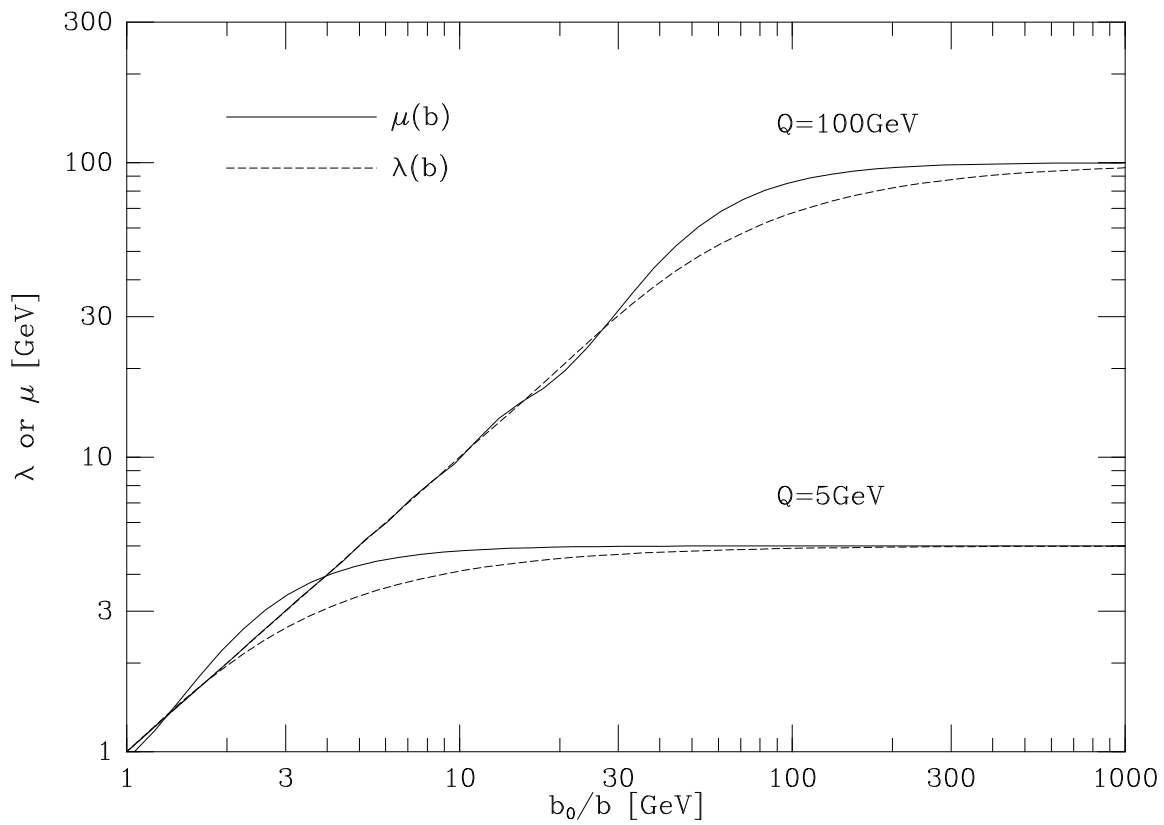


Figure 1: Scales $\mu(b)$ and $\lambda(b)$ compared to b_0/b for $Q = 5, 100$ GeV.

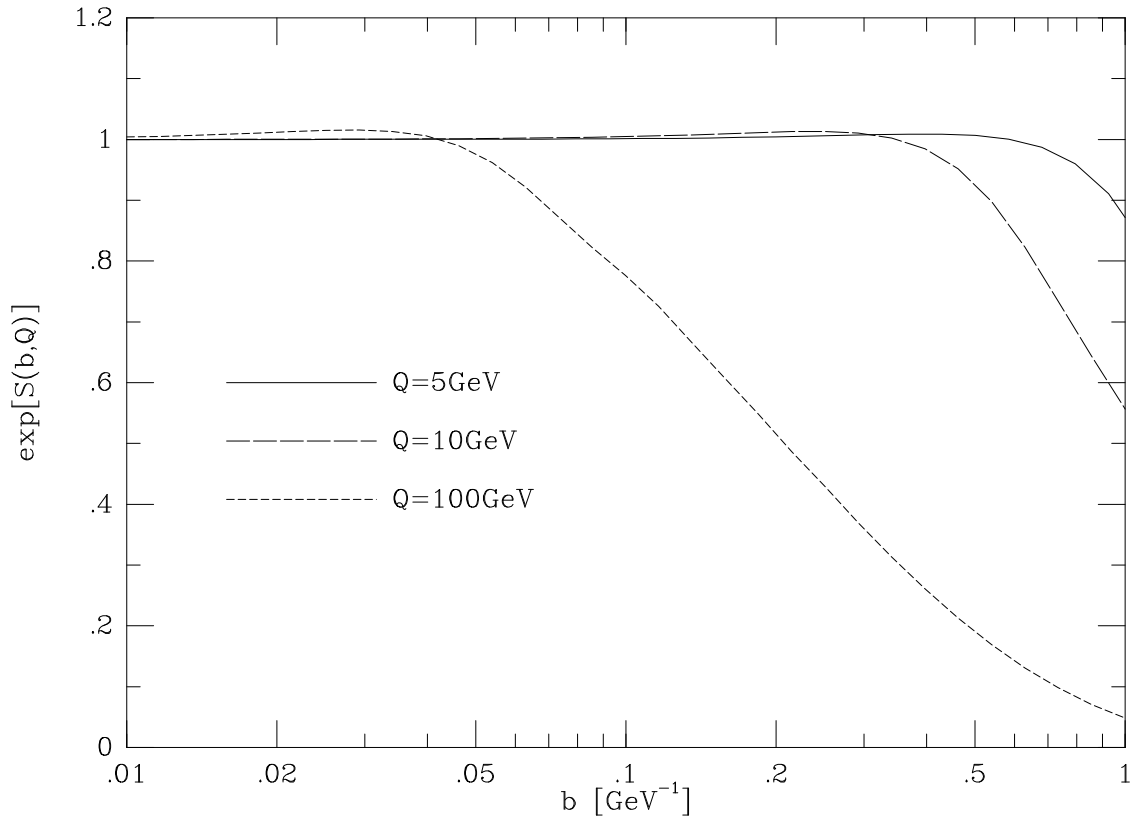


Figure 2: The Sudakov form factor for $Q = 5, 10$ and 100 GeV.

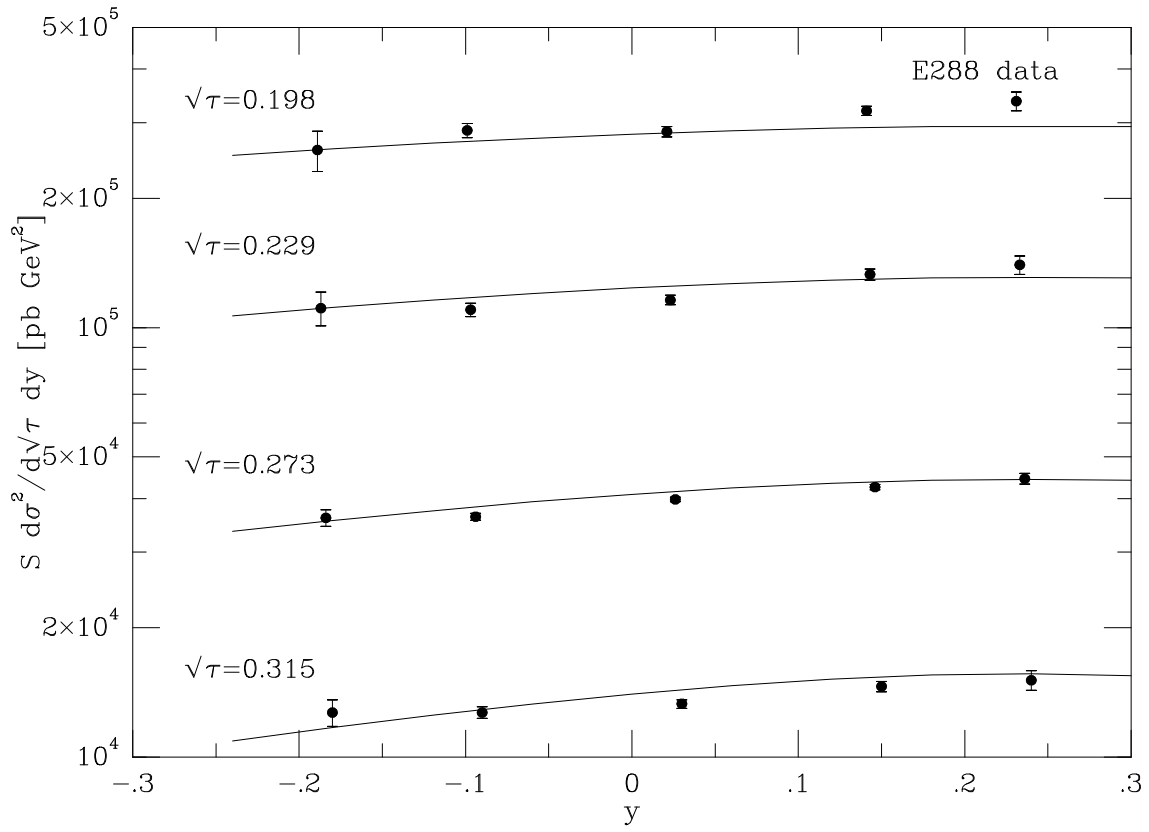


Figure 3: $S d\sigma^2/d\sqrt{\tau} dy$ distribution from E288 compared to theory multiplied by $K = 0.83$.

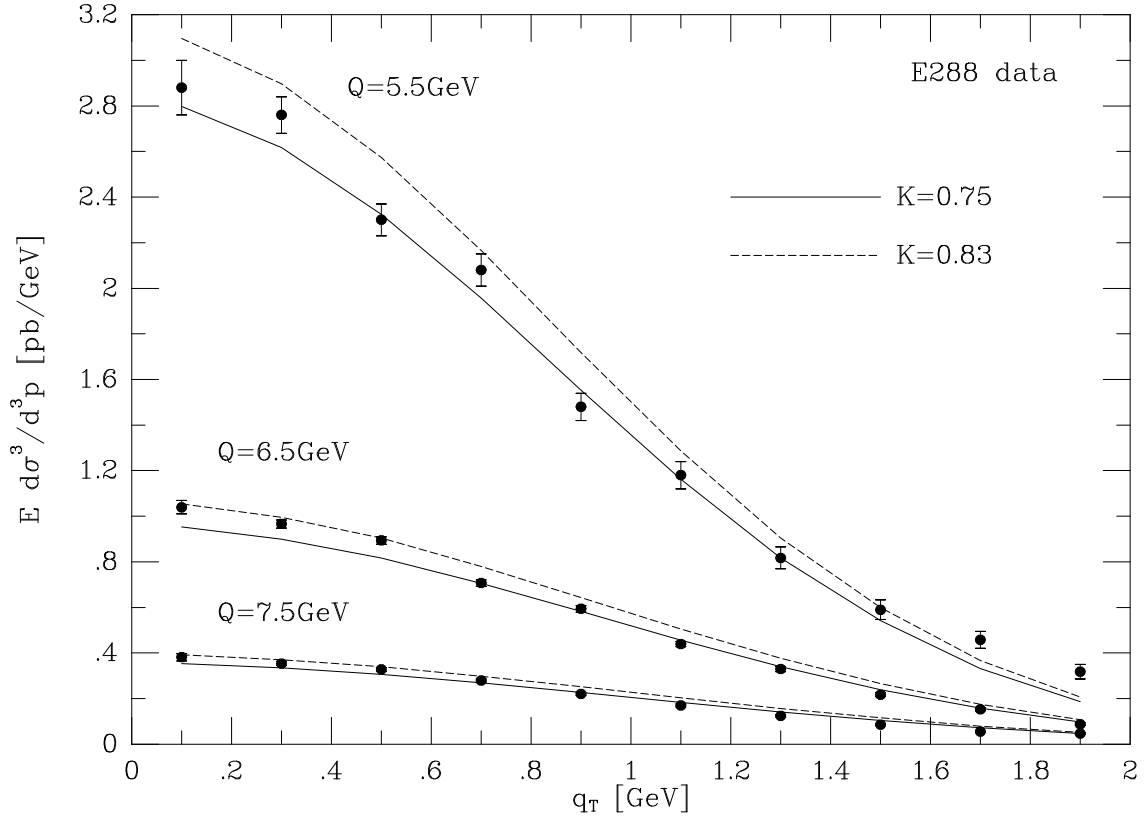


Figure 4: $E \frac{d\sigma^3}{d^3p}$ distribution from E288 compared to theory with $K = 0.75$ (full line) and $K = 0.83$ (dashed line).

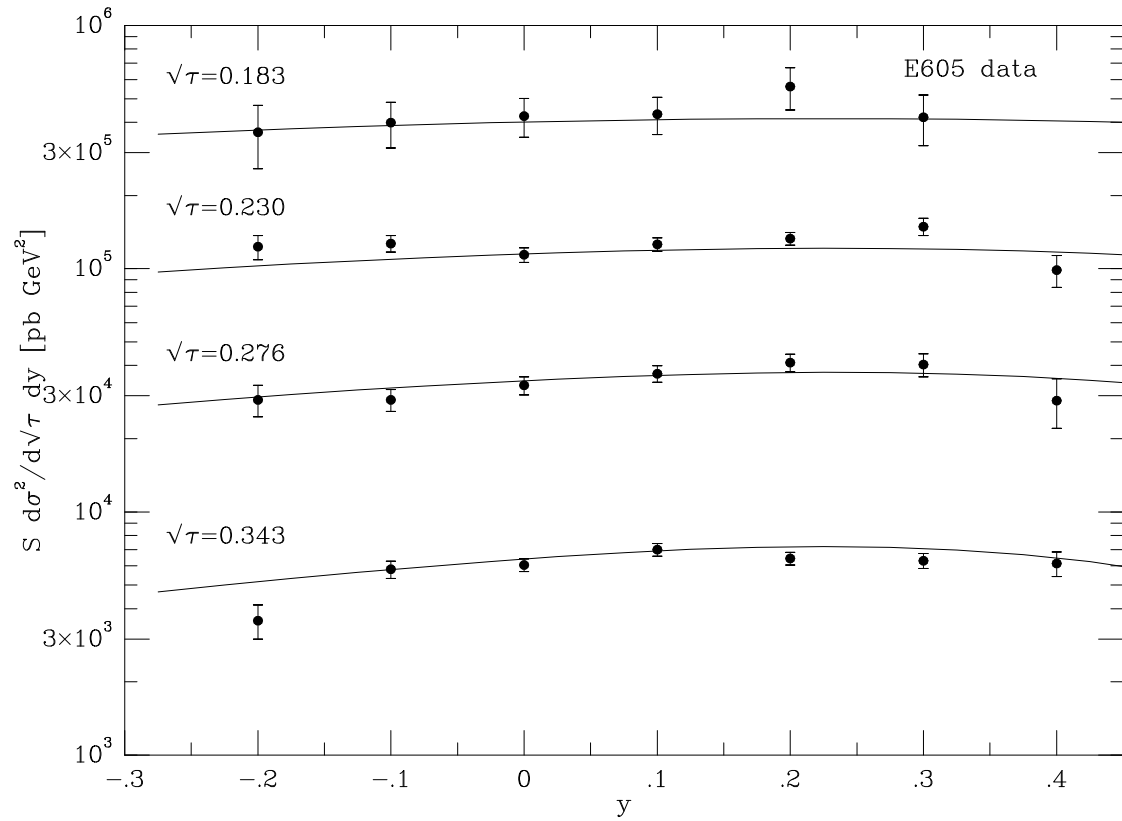


Figure 5: $S \frac{d\sigma^2}{d\sqrt{\tau} dy}$ distribution from E605 compared to theory multiplied by $K = 0.88$.

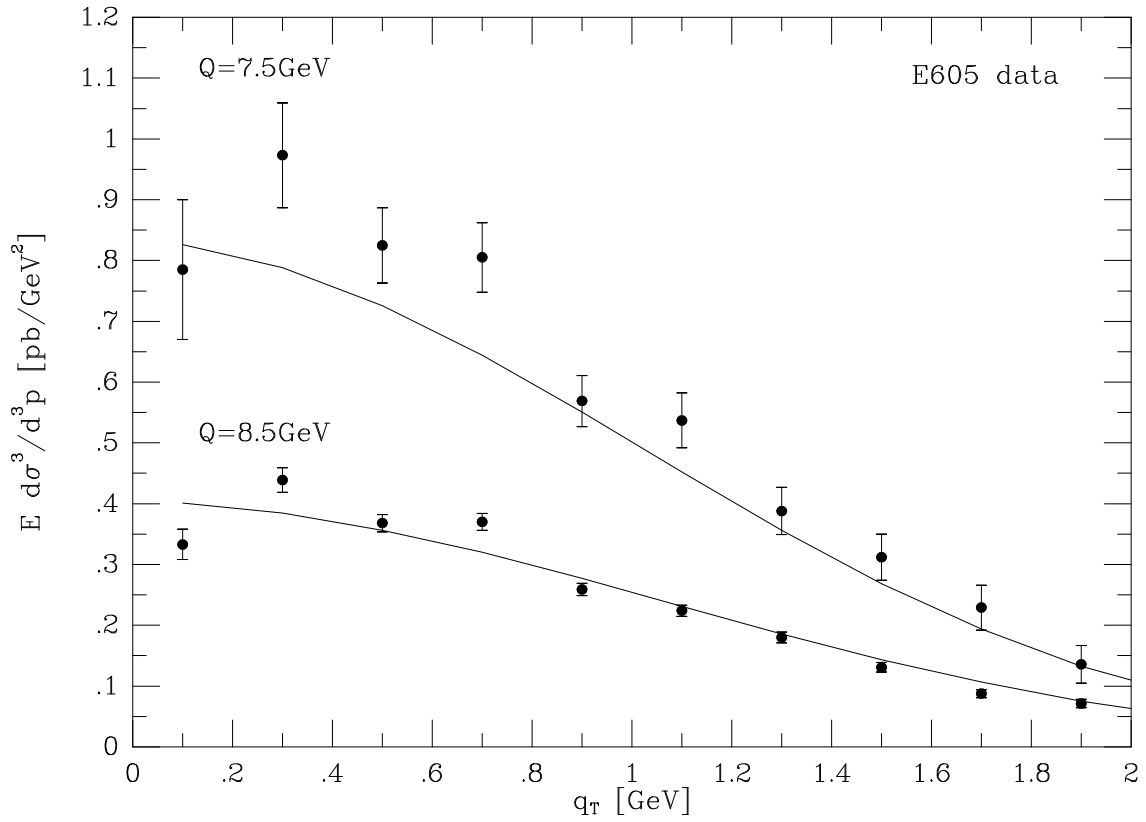


Figure 6: $E \frac{d\sigma^3}{d^3p}$ distribution from E605 (mass bins with $Q < 9 \text{ GeV}$) compared to theory with $K = 0.88$.

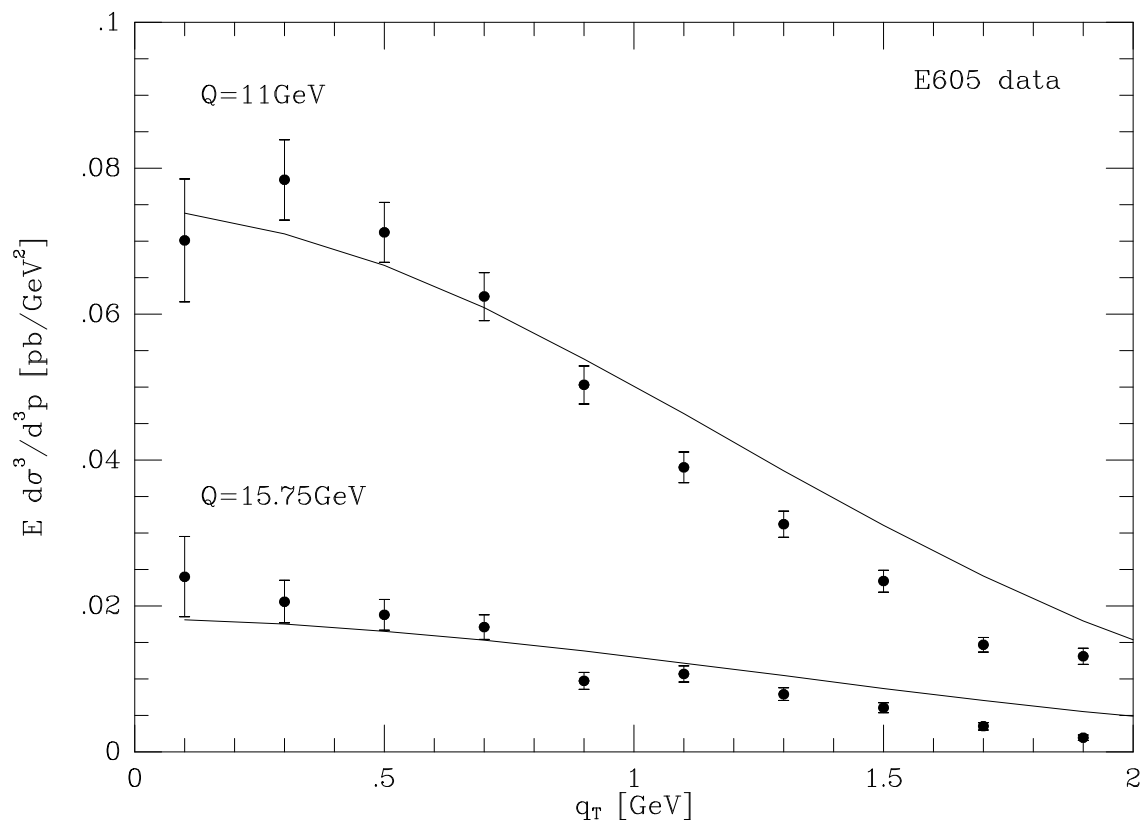


Figure 7: $E \frac{d\sigma^3}{d^3p}$ distribution from E605 (mass bins with $Q > 10.5$ GeV) compared to theory with $K = 0.88$.

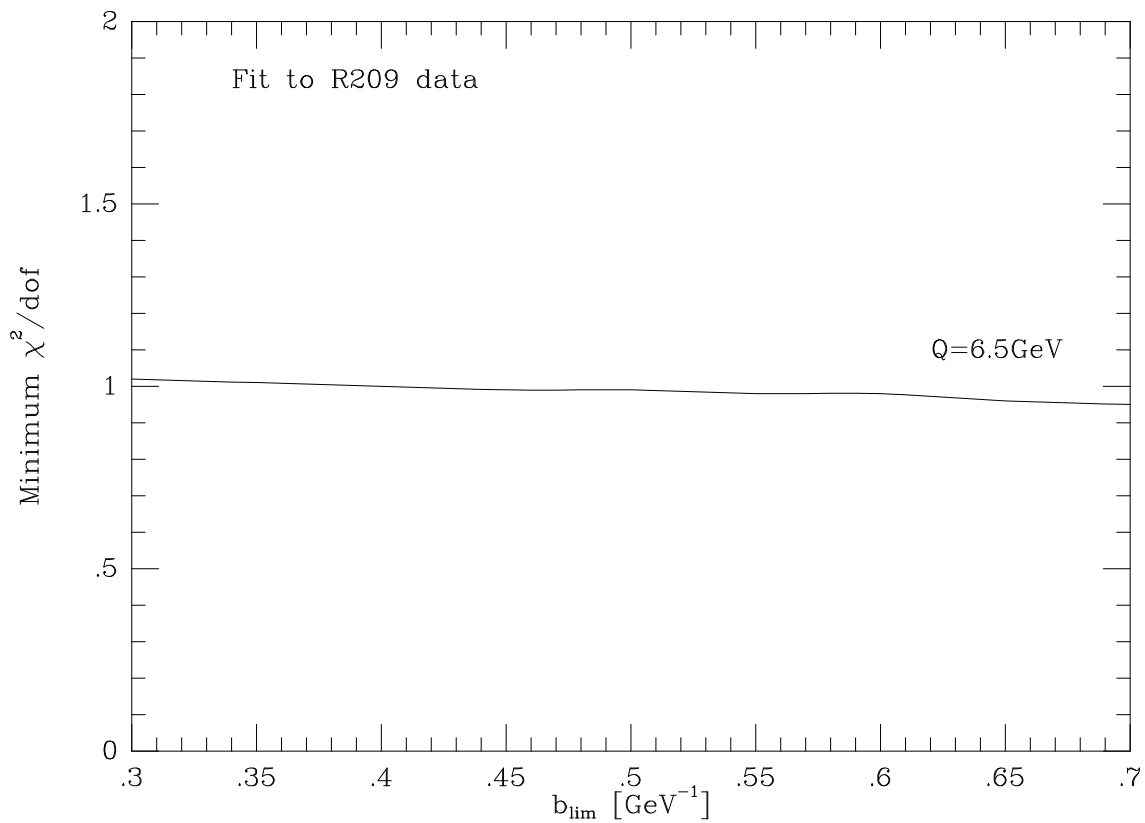


Figure 8: Best χ^2/dof obtained by varying g for R209 data ($5 \text{ GeV} < Q < 8 \text{ GeV}$ and $q_T < 3 \text{ GeV}$). For comparison, with the LY non-perturbative function we obtained χ^2/dof of about 1.3.

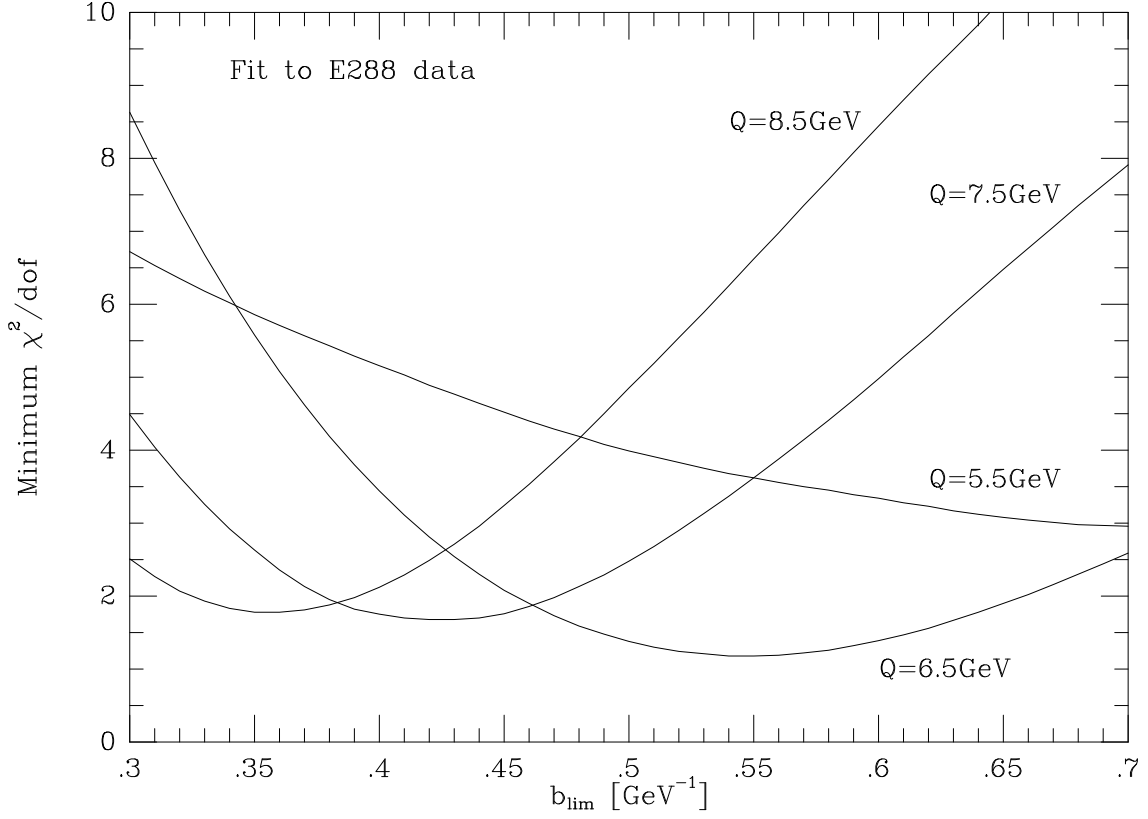


Figure 9: Best χ^2/dof obtained by varying g for E288 data. We used four data sets with $q_T < 2$ GeV and Q below 9 GeV: $5 \text{ GeV} < Q < 6 \text{ GeV}$, $6 \text{ GeV} < Q < 7 \text{ GeV}$, $7 \text{ GeV} < Q < 8 \text{ GeV}$, and $8 \text{ GeV} < Q < 9 \text{ GeV}$. Theoretical results were multiplied by $K = 0.83$. For these data sets the LY form of the non-perturbative function yields χ^2/dof of 6.5, 14.1, 22.9 and 27.5, respectively.

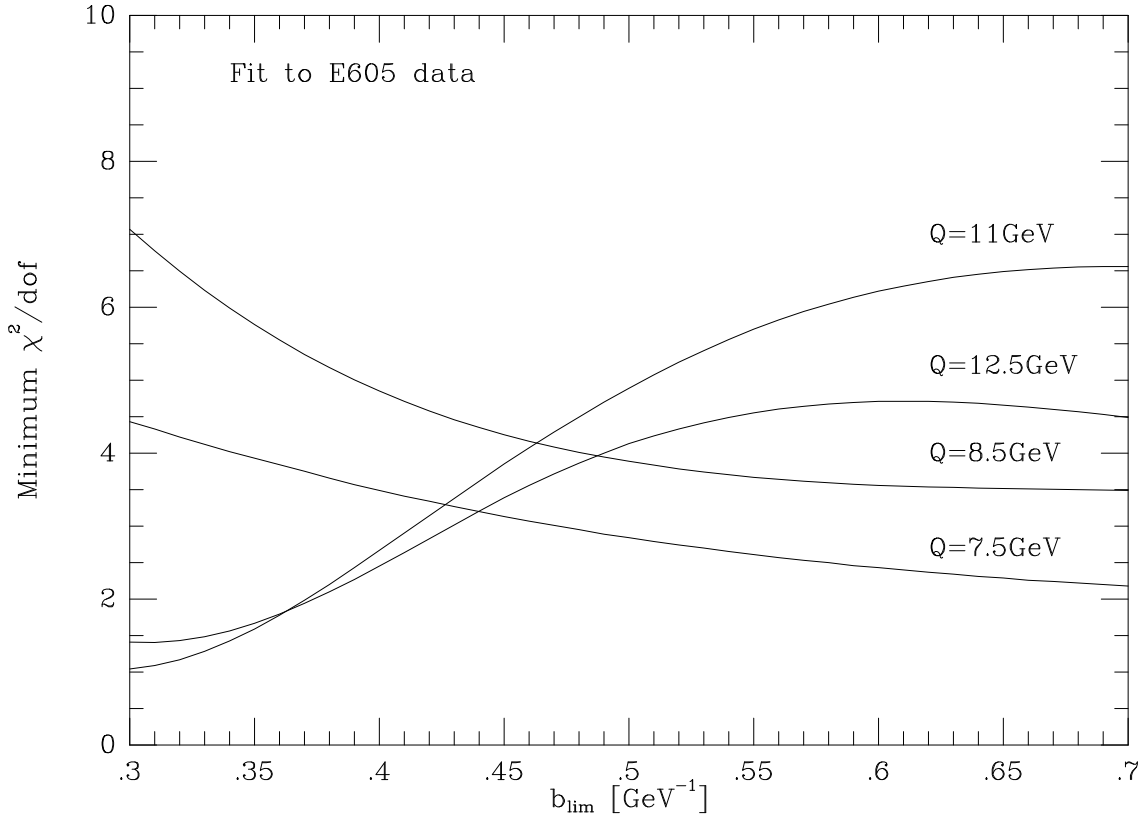


Figure 10: Best χ^2/dof obtained by varying g for E605 data. We used data sets for $7 \text{ GeV} < Q < 8 \text{ GeV}$, $8 \text{ GeV} < Q < 9 \text{ GeV}$, $10.5 \text{ GeV} < Q < 11.5 \text{ GeV}$ and $11.5 \text{ GeV} < Q < 13.5 \text{ GeV}$ (with $q_T < 2 \text{ GeV}$ and $K = 0.88$). For these data sets the LY form of the non-perturbative function yields χ^2/dof of 2.2, 3.5, 16.6 and 17.3, respectively.

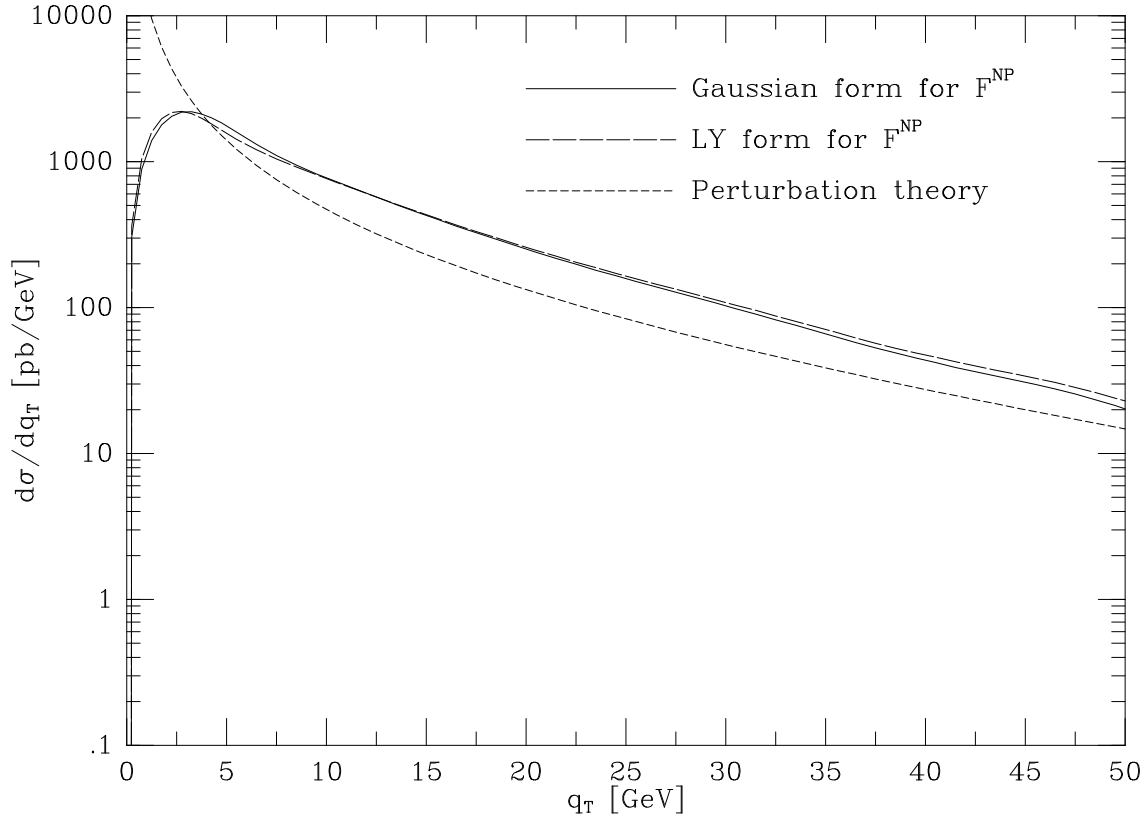


Figure 11: Comparison of the theoretical q_T distributions for $W = W^+ + W^-$ production at Tevatron ($\sqrt{S} = 1.8$ TeV) with $\mathcal{O}(\alpha_S)$ perturbative calculation. These results were obtained with gaussian ($b_{\text{lim}} = 0.5$ GeV $^{-1}$ and $g = 0.33$ GeV 2) and LY form of F^{NP} . We assumed $BR(W \rightarrow e\nu) = 0.111$.

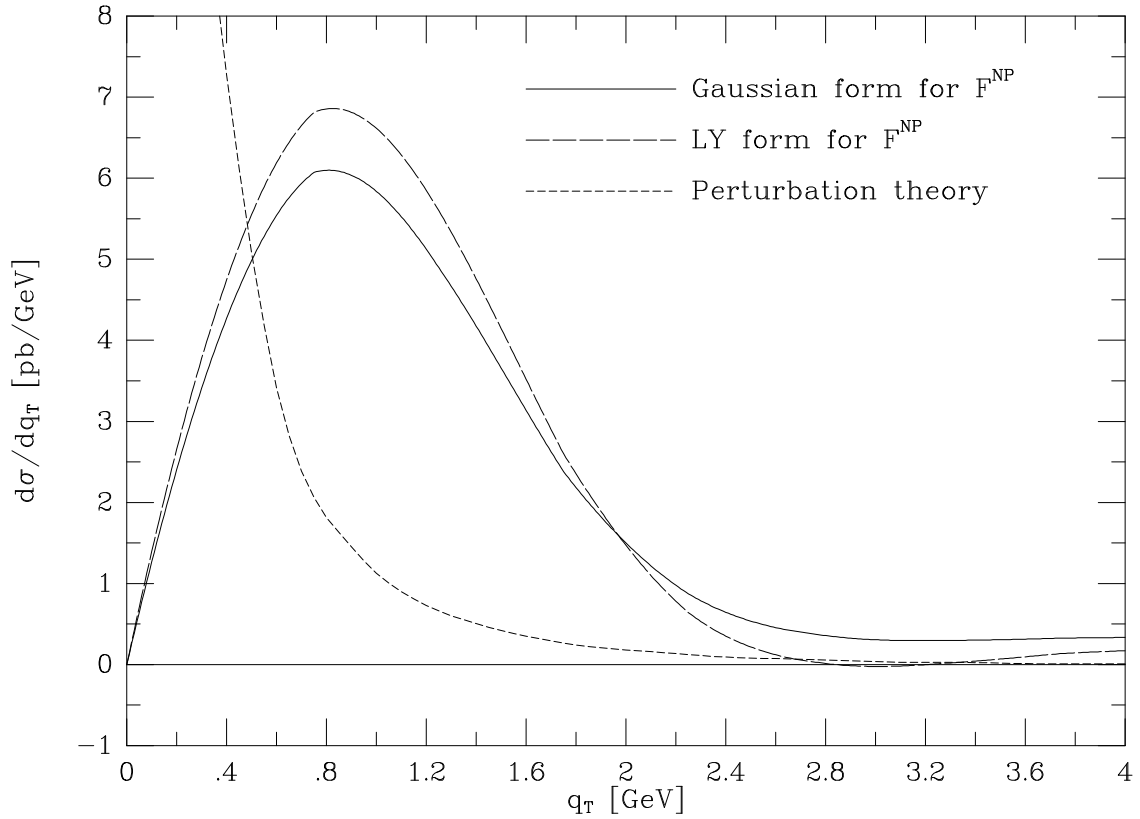


Figure 12: Comparison of the theoretical (resummed plus finite) q_T distributions for E288 experiment ($\sqrt{S} = 27.4$ GeV, $5 \text{ GeV} < Q < 6 \text{ GeV}$ and $-0.27 < y < 0.33$) with $\mathcal{O}(\alpha_S)$ perturbative calculation. These results were obtained with gaussian ($b_{\text{lim}} = 0.5 \text{ GeV}^{-1}$ and $g = 0.33 \text{ GeV}^2$) and LY form of F^{NP} .

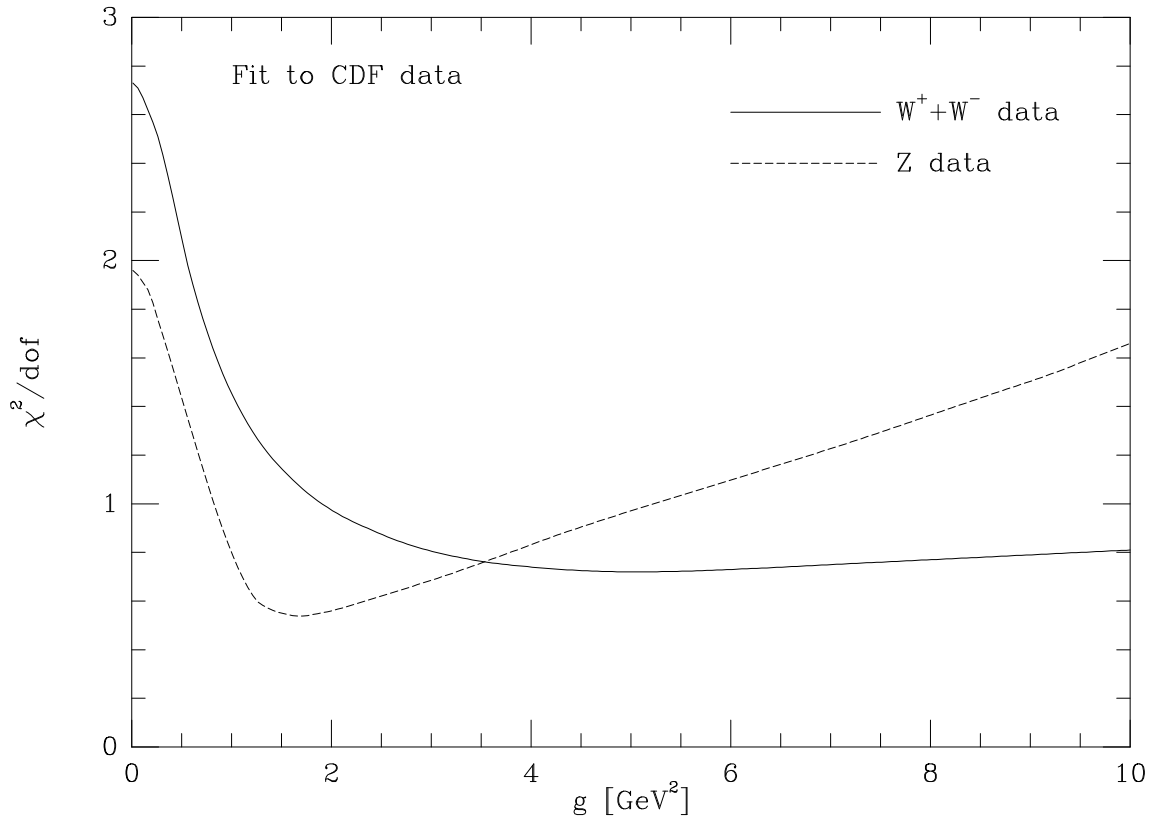


Figure 13: χ^2/dof obtained by varying g for CDF $W^+ + W^-$ (full line) and Z $d\sigma/dq_T$ data (dashed line) below $q_T = 45$ GeV. LY form of the non-perturbative function yields χ^2/dof of about 0.6 and 0.5 for $W^+ + W^-$ and Z data, respectively.

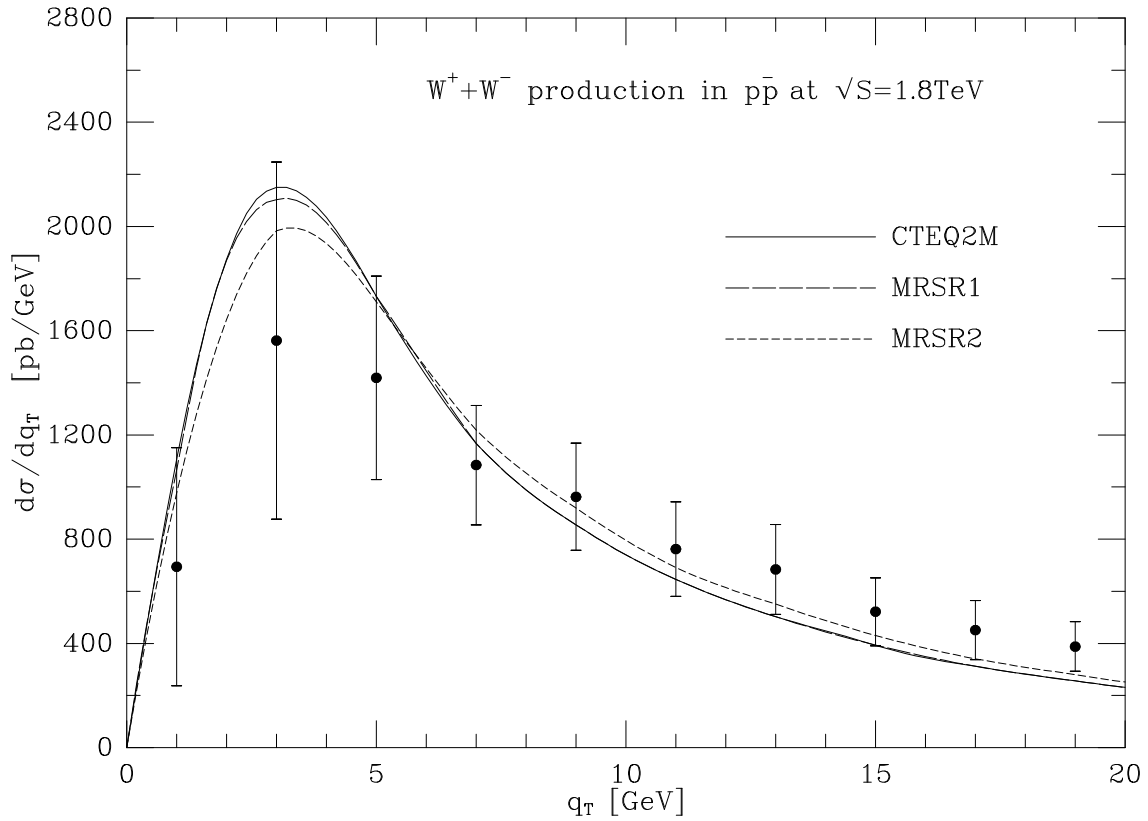


Figure 14: Theoretical prediction for CDF $W^+ + W^-$ $d\sigma/dq_T$ data. These results are obtained using several different parton distribution functions, and with an effective gaussian form of F^{NP} ($g = 3.0 \text{ GeV}^2, b_{\text{lim}} = 0.5 \text{ GeV}^{-1}$).

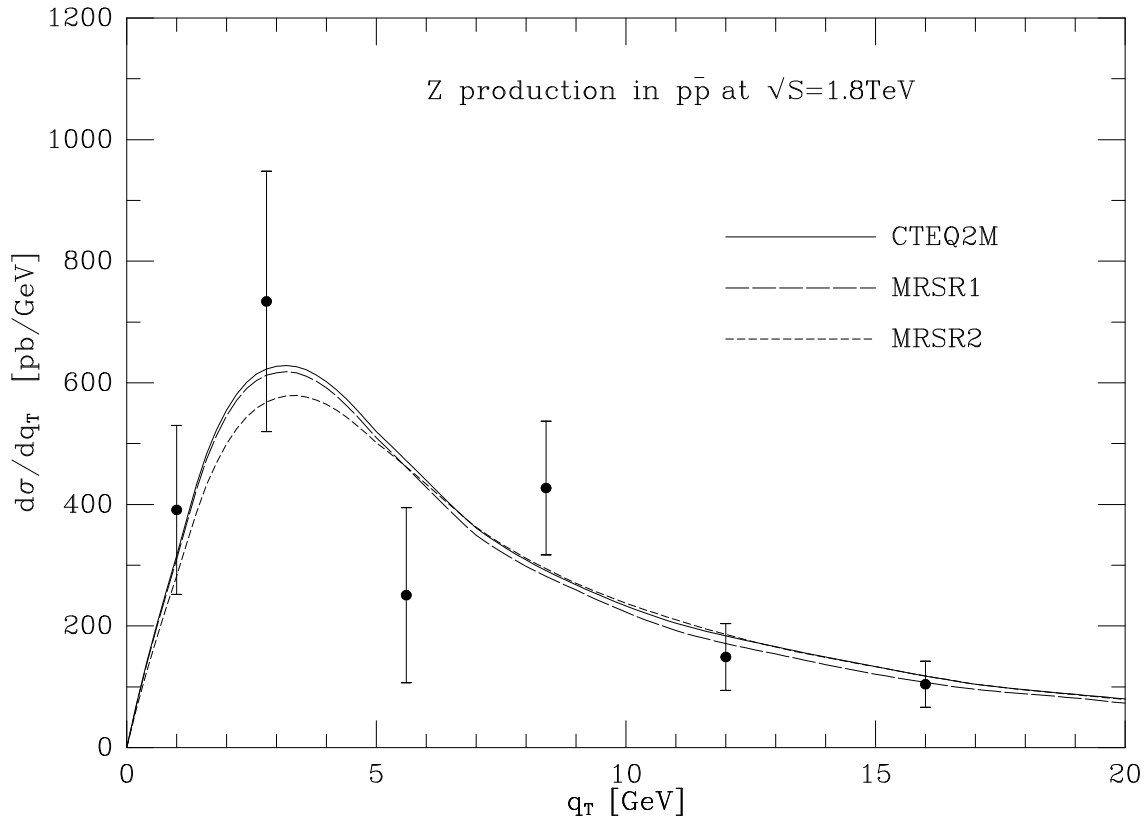


Figure 15: Theoretical prediction for CDF Z $d\sigma/dq_T$. These results are obtained using several different parton distribution functions and with an effective gaussian form of F^{NP} ($g = 3.0 \text{ GeV}^2, b_{\text{lim}} = 0.5 \text{ GeV}^{-1}$).

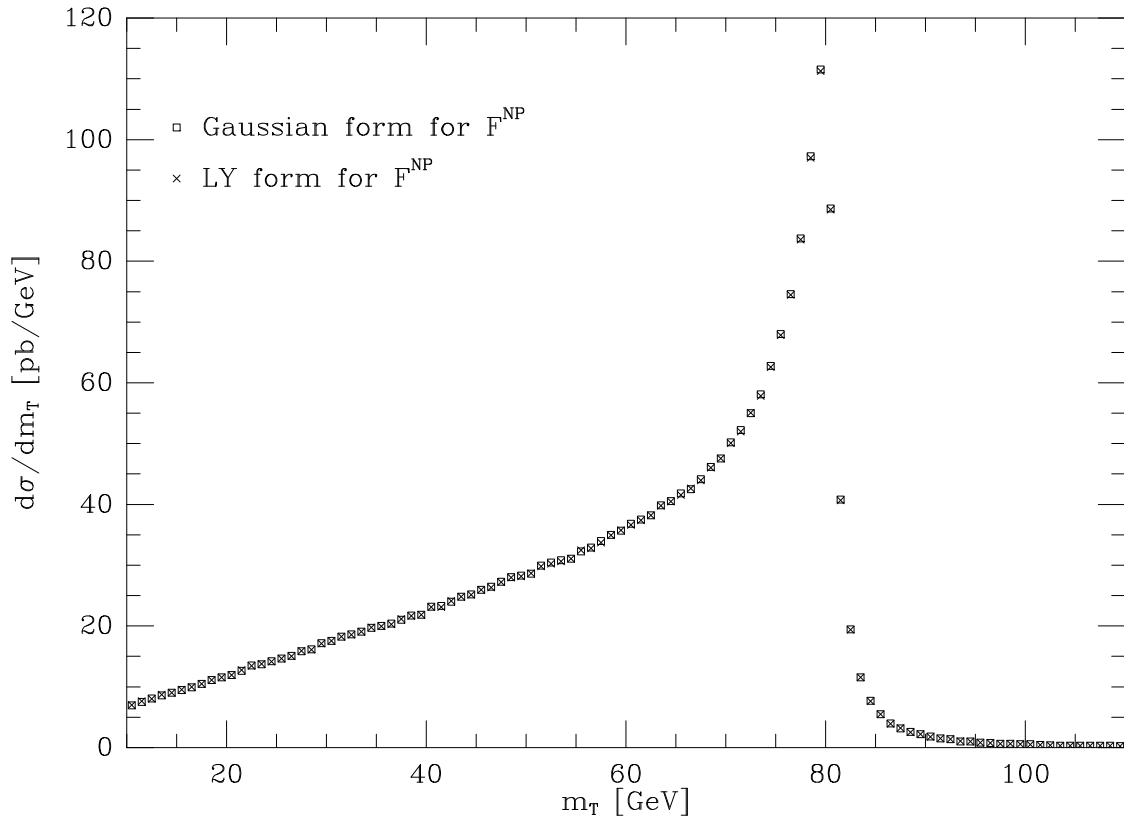


Figure 16: Transverse mass distribution for $W^+ + W^-$ production at Tevatron. We used LY form (with their central values for the non-perturbative parameters), and also an effective gaussian form of F^{NP} (with $g = 3.0 \text{ GeV}^2$ and $b_{\text{lim}} = 0.5 \text{ GeV}^{-1}$).

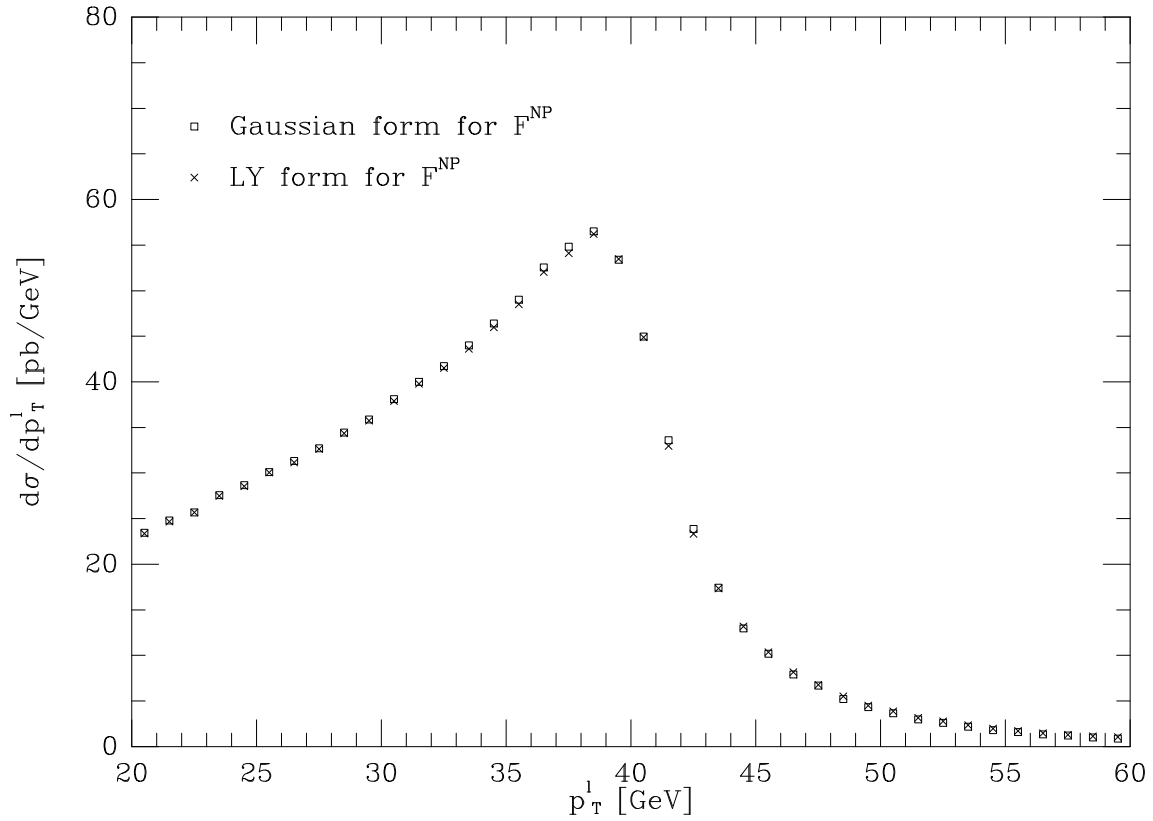


Figure 17: p_T^l distribution from W^- production at Tevatron. We used LY form (with their central values for the non-perturbative parameters), and also an effective gaussian form of F^{NP} (with $g = 3.0 \text{ GeV}^2$ and $b_{\text{lim}} = 0.5 \text{ GeV}^{-1}$).